

**ON THE LOCALIZATION AND DETECTION OF  
MULTIPLE SIGNALS**

**A THESIS SUBMITTED TO THE INSTITUTE OF  
GRADUATE STUDIES  
OF  
NEAR EAST UNIVERSITY**

**By  
AMR ABDELNASER ABDELHAK ABDELBARI**

**In Partial Fulfillment of the Requirements for  
the Degree of Doctor of Philosophy  
in  
Electrical and Electronic Engineering**

**NICOSIA, 2021**

**ON THE LOCALIZATION AND DETECTION OF  
MULTIPLE SIGNALS**

**A THESIS SUBMITTED TO THE INSTITUTE OF  
GRADUATE STUDIES  
OF  
NEAR EAST UNIVERSITY**

**By  
AMR ABDELNASER ABDELHAK ABDELBARI**

**In Partial Fulfillment of the Requirements for  
the Degree of Doctor of Philosophy  
in  
Electrical and Electronic Engineering**

**NICOSIA, 2021**

**Amr Abdelnaser Abdelhak Abdelbari: ON THE LOCALIZATION AND  
DETECTION OF MULTIPLE SIGNALS**

**Approval of Director of Institute of Graduate Studies**

**Prof. Dr. K. Hüsnü Can BAŞER**

**We certify this thesis is satisfactory for the award of the degree of Doctor of  
Philosophy in Electrical and Electronic Engineering**

**Examining Committee in Charge:**

Prof.Dr. Bülent Bilgehan	Committee Chairman, Supervisor, Dean of Engineering Faculty, NEU
Assoc.Prof.Dr. Hüseyin Hacı	Head of Department of Mechatronics, NEU
Assist.Prof.Dr. Ali Serener	Lecturer, Department of Electrical and Elec- tronic Engineering, NEU
Assoc.Prof.Dr. Eser Gemikonaklı	Acting Dean of Faculty of Engineering, Uni- versity of Kyrenia
Assoc.Prof.Dr. Ali Özyapıcı	Lecturer, Department of Mathematics, CIU

I hereby declare that all information in this document has been obtained and presented in accordance with academic rules and ethical conduct. I also declare that, as required by these rules and conduct, I have fully cited and referenced all material and results that are not original to this work.

Name, Last name:

Signature:

Date



## ACKNOWLEDGMENTS

It was a noteworthy years of academic research through my PhD journey. Beginning with the advisory, supervision, and enlightenment role of Prof.Dr. Bülent Bilgehan. His dedication and overwhelming attitude made this academic path easy and straightforward in both research and PhD progresses. No words can express the gratitude I have for him as a mentor, supervisor, and as a scientist. His scholarly advice and life guidance have had a great impact on my way of building critical thinking, approaching research, and accomplishing my thesis.

I owe a deep sense of appreciations to the exceptional researcher Assoc.Prof.Dr. Hüseyin Haci for his enthusiasm and guidance. His timely suggestions and practical ideas have raised my way of conducting research to higher standards and helped me a lot to complete this work.

I would like to express my most sincere gratitude to my adviser, Asst.Prof.Dr. Ali Serener. His continuous support, availability, helping, and understanding have made every phase of the PhD a lot easier. My sincere thanks to all my teachers and colleagues in the Faculty of Engineering, NEU. A special thanks for the great understanding and unconditional support from all my PhD jury members. Their tight but yet in-favor wise decisions were a great attitude and made this accomplishment happened.

Eternally, my deep gratefulness goes to my parents for their unconditional support, end-less love and encouragement. Their insightful thoughts, sacrifices, and continuous prayers have a footprint everywhere in my life. I have no words that can even imagine the deep love they have for me.

Last but not least, my deep sense of gratitude for my beloved wife. Her sense of support, understanding, prompt inspirations, and enthusiasm were beyond the highest sky. Her participation during the study was enormous and without it, I would not be able to complete this work.

To my parents and my wife ...

## ABSTRACT

Signal processing field has been advanced tremendously by the state-of-the-art techniques introduced by array signal processing as the concept of using multiple receivers or array of antenna to process one signal has been investigated and polished over last decades in various aspects regarding the process of any type of signals e.g. electromagnetic, acoustic, medical, and seismic signals. Nevertheless, array of antenna still gain more interests due to its high performance over single antenna in many applications such as radar, sonar, astronomy, wireless communications, and military surveillance. Recently, the usage of array of antenna to localize, detect and decode multiple signals gain a huge attention and many researchers focus on develop such systems for future wireless networks and other applications. However, there are some existing limitations such as the accuracy of localization, the complexity of algorithms as the number of antenna and the number of received signals increases. Also, some localization techniques do not work well in the indoors or require expensive equipment. Interestingly, Direction Of Arrival (DOA) estimation which is one of the main array signal processing branches and widely used in many applications, can be advanced to address the aforementioned problems. As the aims of any localization system are to detect and accurately locate the source of the received signals with low latency.

In this thesis, some new methods have been introduced for unknown wideband signals based on TOPS method. Another contribution is a wideband DOA estimation method based on probabilistic approach which improve the resolution with low complexity. Further, another novel DOA estimation method is introduced for narrowband signals. Since the aim is to practically localize multiple signals with minimum computational costs and estimation error, a full localization approach based on DOA estimation is introduced for both stationary and moving surveillance systems. All these techniques have been tested against the existing to show their performance. The simulation results show a significant improvements that can be deployed in real life applications.

**Keyword:** Array Signal Processing; Direction-Of-Arrival (DOA); Localization algorithm; Probabilistic approach; Unknown signals; Edge detection; wideband signals

## ÖZET

Sinyal işleme alanı, bir sinyali işlemek için birden fazla alıcı veya bir anten dizisi kullanma kavramı olarak, dizi sinyal işleme tarafından sunulan en son teknikler tarafından son on yılda çeşitli yönlerden araştırılmış ve cilalanmıştır. her türlü sinyalin süreci, örneğin elektromanyetik, akustik, tıbbi ve sismik sinyaller. Bununla birlikte, radar, sonar, astronomi, kablosuz iletişim ve askeri gözetleme gibi birçok uygulamada tek antene göre yüksek performansı nedeniyle anten dizisi hala daha fazla ilgi görmektedir. Son zamanlarda, birden fazla sinyali yerleştirmek, algılamak ve kodunu çözmek için anten dizisinin kullanımı büyük bir ilgi görüyor ve birçok araştırmacı gelecekteki kablosuz ağlar ve diğer uygulamalar için bu tür sistemleri geliştirmeye odaklanıyor. Ancak, lokalizasyon doğruluğu, anten sayısı ve alınan sinyal sayısı arttıkça algoritmaların karmaşıklığı gibi bazı sınırlamalar mevcuttur. Ayrıca, bazı yerleştirme teknikleri iç mekanlarda iyi çalışmaz veya pahalı ekipman gerektirir. İlginç bir şekilde, ana dizi sinyal işleme dallarından biri olan ve birçok uygulamada yaygın olarak kullanılan Varış Yönü (DOA) tahmini, yukarıda bahsedilen sorunları gidermek için geliştirilebilir. Herhangi bir yerleştirme sisteminin amacı, alınan sinyallerin kaynağını düşük gecikme ile tespit etmek ve doğru bir şekilde bulmaktır.

Bu tezde, bilinmeyen geniş bant sinyalleri için TOPS yöntemine dayalı bazı yeni yöntemler tanıtılmıştır. Diğer bir katkı, düşük karmaşıklıkla çözünürlüğü iyileştiren olasılıksal yaklaşıma dayalı geniş bantlı bir DOA tahmin yöntemidir. Ayrıca, dar bant sinyalleri için başka bir yeni DOA tahmin yöntemi tanıtılmıştır. Amaç, minimum hesaplama maliyetleri ve tahmin hatası ile birden fazla sinyali pratik olarak lokalize etmek olduğundan, hem sabit hem de hareketli gözetim sistemleri için DOA tahminine dayalı tam bir yerleştirme yaklaşımı tanıtıldı. Tüm bu teknikler, performanslarını göstermek için mevcutlara karşı test edilmiştir. Simülasyon sonuçları, gerçek yaşam uygulamalarında uygulanabilecek önemli iyileştirmeler göstermektedir.

**Anahtar Kelimeler:** Dizi Sinyal İşleme; Varış Yönü (DOA); Yerleştirme algoritması; Olasılıksal yaklaşım; Bilinmeyen sinyaller; Kenar algılama; geniş bant sinyalleri

## CONTENTS

<b>ACKNOWLEDGMENTS .....</b>	<b>v</b>
<b>ABSTRACT.....</b>	<b>vii</b>
<b>ÖZET.....</b>	<b>viii</b>
<b>LIST OF TABLES .....</b>	<b>xi</b>
<b>LIST OF FIGURES.....</b>	<b>xii</b>
<b>LIST OF ABBREVIATIONS AND SYMBOLS .....</b>	<b>xiv</b>
<b>CHAPTER 1: INTRODUCTION</b>	
1.1 Previous Work .....	3
1.1.1 Wideband DOA estimation .....	3
1.1.2 Narrowband DOA estimation .....	5
1.2 Scope and Contributions of The Thesis .....	6
1.3 List of Publications.....	7
<b>CHAPTER 2: NEW WIDEBAND DOA ESTIMATION TECHNIQUES</b>	
2.1 Introduction.....	9
2.2 Signal Model .....	9
2.3 Conventional DOA Estimation Methods.....	11
2.3.1 IMUSIC .....	11
2.3.2 TOPS .....	12
2.3.3 Squared-TOPS .....	13
2.3.4 Weighted squared TOPS .....	14
2.4 MNS-TOPS.....	15
2.4.1 Signal Detection .....	16
2.4.2 Proposed methodology .....	18
2.4.3 Simulation results .....	21

2.4.4	Conclusion .....	26
2.5	PESO .....	28
2.5.1	Introduction .....	28
2.5.2	The Proposed method .....	29
2.5.3	Simulation results .....	34
2.5.4	Conclusion .....	38
<b>CHAPTER 3: NEW NARROWBAND DOA ESTIMATION TECHNIQUES</b>		
3.1	Introduction.....	39
3.2	Signal Model .....	40
3.3	Conventional DOA Estimation Methods .....	41
3.3.1	MUSIC.....	41
3.3.2	ESPRIT .....	42
3.3.3	Capon .....	43
3.3.4	PM.....	43
3.4	The Proposed Method.....	44
3.4.1	PRESS DOA Estimation Method.....	44
3.4.2	Localization Algorithm .....	45
3.4.3	The PRESS algorithm .....	47
3.5	Simulation Results .....	48
3.6	Conclusion.....	52
<b>CHAPTER 4: CONCLUSIONS AND FUTURE WORK</b>		
4.1	Conclusions.....	53
4.2	Future Work .....	54
<b>REFERENCES .....</b>		<b>55</b>
<b>APPENDICES</b>		
Appendix 1: CURRICULUM VITAE.....		64
Appendix 2: Similarity Report .....		68

## LIST OF TABLES

<b>Table 2.1:</b> Simulation cases. ....	21
<b>Table 2.2:</b> The complexity of common mathematical multiplications and stages used within DOA algorithms.....	26
<b>Table 3.1:</b> Bias of PRESS method at -5dB for the three sources measured from three separated locations. ....	51

## LIST OF FIGURES

<b>Figure 2.1:</b> Visual illustration of the edge detection process.....	16
<b>Figure 2.2:</b> The proposed algorithm.....	19
<b>Figure 2.3:</b> Edge detection stage (a) shows the frequency spectrum of interest and (b) shows the output of the edge detection. ....	20
<b>Figure 2.4:</b> Spatial spectrum at SNR = -5 dB for the four simulation cases, where (a) $M = 10, D = 3$ at $(20^\circ \ 40^\circ \ 65^\circ)$ and $L = 26$ ; (b) $M = 8, D = 3$ at $(20^\circ \ 40^\circ \ 65^\circ)$ and $L = 26$ ; (c) $M = 10, D = 3$ at $(20^\circ \ 40^\circ \ 80^\circ)$ and $L = 16$ ; and (d) $M = 10, D = 5$ at $(-10^\circ \ 7^\circ \ 30^\circ \ 65^\circ \ 80^\circ)$ and $L = 26$ . ..	22
<b>Figure 2.5:</b> RMSE of all three estimated sources for the three simulation cases, where (a) $M = 10, D = 3$ at $(20^\circ \ 40^\circ \ 65^\circ)$ and $L = 26$ ; (b) $M =$ $8, D = 3$ at $(20^\circ \ 40^\circ \ 65^\circ)$ and $L = 26$ ; and (c) $M = 10, D = 3$ at $(20^\circ \ 40^\circ \ 80^\circ)$ and $L = 16$ . ....	23
<b>Figure 2.6:</b> Bias of the first source at $20^\circ$ for the three simulation cases, where (a) $M = 10, D = 3$ at $(20^\circ \ 40^\circ \ 65^\circ)$ and $L = 26$ ; (b) $M = 8, D = 3$ at $(20^\circ \ 40^\circ \ 65^\circ)$ and $L = 26$ ; and (c) $M = 10, D = 3$ at $(20^\circ \ 40^\circ \ 80^\circ)$ and $L = 16$ .....	24
<b>Figure 2.7:</b> Bias of the second source at $40^\circ$ for the three simulation cases, where (a) $M = 10, D = 3$ at $(20^\circ \ 40^\circ \ 65^\circ)$ and $L = 26$ ; (b) $M = 8, D = 3$ at $(20^\circ \ 40^\circ \ 65^\circ)$ and $L = 26$ ; and (c) $M = 10, D = 3$ at $(20^\circ \ 40^\circ \ 80^\circ)$ and $L = 16$ .....	25
<b>Figure 2.8:</b> Mean execution time elapsed by each simulation cases, where (a) $M = 10, D = 3$ at $(20^\circ \ 40^\circ \ 65^\circ)$ and $L = 26$ ; (b) $M = 8, D = 3$ at $(20^\circ \ 40^\circ \ 65^\circ)$ and $L = 26$ ; and (c) $M = 10, D = 3$ at $(20^\circ \ 40^\circ \ 80^\circ)$ and $L = 16$ .....	27
<b>Figure 2.9:</b> The selective indicator of all three estimated sources for the three simulation cases, where 1st case: $M = 10, D = 3$ at $(20^\circ \ 40^\circ \ 65^\circ)$ and $L = 26$ ; 2nd case: $M = 8, D = 3$ at $(20^\circ \ 40^\circ \ 65^\circ)$ and $L = 26$ ; and 3rd case: $M = 10, D = 3$ at $(20^\circ \ 40^\circ \ 80^\circ)$ and $L = 16$ .....	28



<b>Figure 2.10:</b> Visual illustration of the probability of detected peaks within the spatial spectrum of all frequency bins.....	31
<b>Figure 2.11:</b> Normalized spatial spectrum at (a) -5 dB, and (b) -2.5 dB SNR for PESO compared with IMUSIC and TOPS methods for sources at at $30^\circ$ , $50^\circ$ and $65^\circ$ . ....	33
<b>Figure 2.12:</b> The probability of resolution for proposed method PESO compared with IMUSIC and TOPS methods. ....	34
<b>Figure 2.13:</b> Total RMS Error for all three detected wideband sources at $30^\circ$ , $50^\circ$ and $65^\circ$ . ....	35
<b>Figure 2.14:</b> Bias of the sources at (a) $30^\circ$ , (b) $50^\circ$ , and (c) $65^\circ$ for the proposed method PESO, IMUSIC and TOPS methods. ....	36
<b>Figure 2.15:</b> Mean consumed time for 200 simulation rounds by the calculations of the proposed method PESO, IMUSIC and TOPS methods.....	37
<b>Figure 3.1:</b> Visual illustration of localization algorithm using 3 arrays to locate two sources. S1 and S2 are the locations of the sources 1 and 2 respectively. $\theta_{1,a1}$ and $\theta_{2,a1}$ are the estimated DOA at the first array from the S1 and S2, respectively. $\theta_{1,a2}$ and $\theta_{2,a2}$ are the estimated DOA at the second array from the S1 and S2, respectively. $\theta_{1,a3}$ and $\theta_{2,a3}$ are the estimated DOA at the third array from the S1 and S2, respectively. ....	45
<b>Figure 3.2:</b> Normalized spatial spectrum at -5dB for PRESS, MUSIC, PM, and Capon methods for sources at $26^\circ$ , $30^\circ$ , $45^\circ$ , $53^\circ$ , and $60^\circ$ .....	47
<b>Figure 3.3:</b> Total RMSE measured from -5dB to 25dB values of SNR for PRESS, MUSIC, TLS-ESPRIT, PM, and Capon methods for five sources located at $26^\circ$ , $30^\circ$ , $45^\circ$ , $53^\circ$ , and $60^\circ$ . ....	48
<b>Figure 3.4:</b> Bias of the source at: (a) $26^\circ$ , (b) $30^\circ$ , and (c) $60^\circ$ , for PRESS, MUSIC, and TLS-ESPRIT methods. ....	49
<b>Figure 3.5:</b> The case study of localization algorithm in which it locates three sources at three different locations using three arrays. ....	50

## LIST OF ABBREVIATIONS AND SYMBOLS

<b>AIC</b>	Akaike Information Criterion
<b>AOA</b>	Angle of Arrival
<b>AWGN</b>	Additive White Gaussian Noise
<b>CSS</b>	Coherent Signal Subspace
<b>CSSM</b>	Coherent Signal Subspace Method
<b>DOA</b>	Direction of Arrival
<b>DSP</b>	Digital Signal Processing
<b>ESPRIT</b>	Estimation of Signal Parameters via Rotational Invariance Technique
<b>EVD</b>	Eigen Value Decomposition
<b>FFT</b>	Fast Fourier Transform
<b>GPS</b>	Global Positioning System
<b>IMUSIC</b>	Incoherent Multiple Signal Parameter Estimation
<b>LS-ESPRIT</b>	Least square-ESPRIT
<b>MATLAB</b>	Mathematical Laboratory
<b>MDL</b>	Minimum Description Length
<b>MNS-TOPS</b>	Minimum Noisy Subband-TOPS
<b>MSC</b>	Mean Shifted Clustering
<b>MUSIC</b>	Multiple Signal Parameter Estimation
<b>PESO</b>	Probabilistic Evaluation of Subspaces Orthogonality
<b>PM</b>	Propagator Method

<b>PRESS</b>	Probabilistic Estimation of Several Signals
<b>PSD</b>	Power Spectrum Density
<b>RMSE</b>	Root Mean Square Estimate
<b>RSS</b>	Received Signal Strength
<b>SB-TOPS</b>	Subbands-Based-TOPS
<b>SNR</b>	Signal-to-Noise Ratio
<b>SupSVD</b>	Supervised Singular Value Decomposition
<b>SVD</b>	Singular Value Decomposition
<b>TDOA</b>	Time Difference of Arrival
<b>TLS-ESPRIT</b>	Total Least Square-ESPRIT
<b>TOA</b>	Time of Arrival
<b>TOPS</b>	Test of Orthogonality of Projected Subspaces
<b>UAV</b>	Unmanned Aerial Vehicle
<b>ULA</b>	Uniform Linear Array
<b>WAVES</b>	Weighted Average of Signal Subspace
<b>WSF</b>	Weighted subspace Fitting
<b>WSNs</b>	Wireless Sensor Networks
<b>WS-TOPS</b>	Weighted Squared-TOPS
<b>A</b>	Matrix of Steering Vectors
<b><math>\mathbb{C}^n</math></b>	Complex Number Space
<b><math>\mathbf{E}\{\cdot\}</math></b>	The Statistical Expectation
<b><math>\mathbf{E}_s</math></b>	The Signal Subspace Eigenvectors

$\mathbf{E}_n$	The Noise Subspace Eigenvectors
$\mathbf{F}(\theta)$	The Spatial Spectrum
$\mathbf{I}$	The Identity Matrix
$\mathbf{O}(\cdot)$	Big-O notation
$\mathbf{P}_{ss}$	Signal Correlation Matrix
$\mathbf{range}\{\cdot\}$	Range of Matrix
$\mathbf{V}_{xx}$	The Covariance Matrix
$\lambda$	Wavelength
$\Phi$	Spatial Frequency
$\theta$	Angle of Arrival
$\sigma^2$	Noise Variance
$\phi$	Search Angle

# CHAPTER 1

## INTRODUCTION

Signals by the mean of any source, shape or expression, are in every side of our lives as well as in nature from electromagnetic, acoustics, and seismic waves to medical signals, cosmic and gravitational waves. Understanding the related phenomenons and the characteristics of each kind of signals helped the human kind tremendously. Consequently, the ever growing applications around us that make our daily life more comfortable and advanced are somehow based on that basic understanding. However, the more the technology advanced, the more need for deep research on the sources of signals to resolve many unsolved and ambiguous problems. Therefore, the research still needed to apply new techniques on the understanding of the nature of signals and their origins (Haykin & Veen, 2002).

One of the important questions about any type of signal is the location of its source which lead to the characteristics of that source. Localization of signal's source introduces various challenging issues such as the strength of the received signal, the effect of the channel on the signal, the existence of noise, the interference of other signals, the multi-path fading, and the sensing for the signal on the desired spectrum. To address these problems, many locating techniques have been proposed and widely used for decades e.g. Time of Arrival (TOA), Time Difference of Arrival (TDOA), Angle of Arrival (AOA), Received Signal Strength (RSS), Global Positioning System (GPS), . . . , etc. In general, localization techniques can be classified to (Obeidat, Shuaieb, Obeidat, & Abd-Alhameed, 2021; Xiao & Zeng, 2020):

- Active localization system which sends signals to identify the location of the target e.g. Radar, and Sonar systems.
- Cooperative localization where the target cooperates with the system or multiple reciprocals detect and cooperate to estimate the location of the target e.g. cellular network and GPS system.
- Passive localization in which the system estimate the location by observing the signals

that imaging on the antenna at the time of observation e.g. TOA and RSS.

- Blind localization where the system localizes an unknown target or signal emitting source. e.g. Direction of Arrival (DOA).

Localization is very important topic in wireless communication systems (del Peral-Rosado, Raulefs, López-Salcedo, & Seco-Granados, 2018; Munir, Zahoor, Rahim, Lagrange, & Lee, 2018). Number of researchers highlighted the importance of localization as in the geographical routing (Karp & Kung, 2000), geographic key distribution (D. Liu & Ning, 2003), and location-based identification (Sastry, Shankar, & Wagner, 2003). There are many applications relying on the accuracy of the localization such as intruder or jammer identification, environmental monitoring, health monitoring and object tracking (P. Zhang, Lu, Wang, & Wang, 2017; Akyildiz, Su, Sankarasubramaniam, & Cayirci, 2002). The location estimation becomes more important in military applications where incorrect estimation of the location leads to severe damages (Zeng, Cao, Hong, Zhang, & Xie, 2013). Moreover, localization is one of the most important topics in Wireless Sensor Networks (WSNs) since many fundamental techniques in WSNs, e.g., geographical routing (Karp & Kung, 2000), geographic key distribution (D. Liu & Ning, 2003), and location-based authentication (Sastry et al., 2003) require the positions of unknown nodes. Also, the positions of unknown nodes play a critical role in many WSNs applications, such as monitoring applications include environmental monitoring, health monitoring, and tracking applications include tracking objects, animals, humans, and vehicles (Akyildiz et al., 2002). When a WSN is deployed in hostile environments, it is vulnerable to threats and risks. Many attacks exist, e.g., wormhole, sinkhole and Sybil attacks, to make the estimated positions incorrect. Specifically for some applications, e.g., military applications like battlefield surveillance or environmental applications like forest fire detection (Zeng et al., 2013), incorrect positions may lead to severe consequences, e.g., wrong military decisions on the battlefield and false alarms to people. Hence, the issues of secure localization must be addressed in WSNs (Hehdly, Laaraiedh, Abdelkefi, & Siala, n.d.).

DOA estimation is one of the main application of the signal processing sub-field array signal processing which concerns about using array of sensors instead of single sensor. The

advantages of using array of sensors over single sensor include beamforming, higher gain at lower signal strength levels (low Signal-to-noise ratio (SNR)), exploiting more parameters, introducing new dimensions on the extracted data which allow for combining techniques, and higher throughput of the overall communication system (Monzingo, Haupt, & Miller, 2011). The applications of array signal processing extend to wireless communication networks, radar system, sonar system, medical field, civil surveillance, seismic exploration, and military applications (Rudnitskaya, 2019; Turqueti, Oruklu, & Saniie, 2014; Nicoliche, Oliveira, & Lima, 2020; Balanis, 2007). In this thesis, the first part focuses on the DOA estimation using an array of antenna as its one of the promising techniques in the localization of multiple sources especially the closely related sources (Abdelbari, 2018).

In this chapter, the previous works on DOA estimation techniques are presented to highlight the recent work and clarify the problems still need for further research. Then, the aims and scientific contributions of the Ph.D. thesis which concentrates on introducing some new techniques and technologies in both localization and detection of multiple signals. Finally, some parts of this thesis have been published in international journals and presented in international conferences which listed on the list of publications. Beside the work included on the thesis, the list includes other published research works that have been conducted during the Ph.D. program duration.

## **1.1 Previous Work**

In this section, we briefly review the literature on both DOA estimation methods to state the well-known works and highlight recent developments. This should give a deep insight about the limitations and challenges that can be studied in further research and outline the scope and contributions of this thesis in the following section.

### **1.1.1 Wideband DOA estimation**

The wideband signals are applicable in a wide range of electric field as in radar, sonar, seismic, mobile communication, biomedical engineering and military surveillance (Wan, Han, Shu, Chan, & Zhu, 2016). For instance, 5th Generation (5G) networks will demand high accuracy in the localization techniques for outdoor and indoor environments. The localization

of wideband sources is very much different than the narrowband signals. The classical DOA estimation methods that applied to narrowband DOA estimation cannot be applied directly to wideband signals (Aboutanios, Hassanien, El-Keyi, Nasser, & Vorobyov, 2017). The difference is due to the phase difference between the antenna array sensors and the temporal frequency (Bilgehan & Abdelbari, n.d.). The signals in wideband analysis require a pre-processing stage at the signal decomposition level. Generally, the wideband signal is applied to the filter bank or Fast Fourier Transform (FFT) to decompose the signal into a set of narrowband subbands for further analysis (J. Wang, Zhao, & Wang, 2008). There are two types of DOA estimation algorithms applicable to the decomposition process. The algorithms are known as the incoherent signal subspace method (ISSM) (J. Zhang, Dai, & Ye, 2010) and the coherent signal subspace method (CSSM) (Kulhandjian, Kulhandjian, Kim, & D'Amours, 2018). The characteristics of the ISSM method allows the decomposition of a wideband into narrowband and uses all subbands equally in processing. The major drawback of this method is that it produces inaccurate results at low SNR values. The disadvantage of the ISSM method arises due to poor signal estimation in the subbands (Ebadi & Moghaddam, 2017).

The CSSM method was introduced to eliminate such problems encountered by the ISSM method (Yoon, Kaplan, & McClellan, 2006). The improvement in the CSSM method is due to the correlation matrix of each frequency band handled by the transformation matrices (Ebadi & Moghaddam, 2017). Another improvement is because the focused matrices are averaged to generate a new correlation matrix. There are many techniques available to obtain the focusing matrix (Yu, Liu, Huang, Zhou, & Xu, 2007). The classical methods have an important drawback at an initial processing stage that requires some reference values related to the signal. This requires prior knowledge of the direction of the emitted signal. The estimation may end up to be far from the real source location. Another possible method is the weighted average of signal subspaces (WAVES) that requires suitable initial values and has a good performance based on the accurate selection of the initial values (di Claudio & Parisi, 2001). The problem of the initial estimation attempted to be resolved using the test of the orthogonality of projected subspaces (TOPS) and its further improvements. The introduced method overcomes the problem with the initial assumptions but generated new



problems due to the false peaks encountered as a valuable signal source (Hayashi & Ohtsuki, 2016).

### **1.1.2 Narrowband DOA estimation**

The significance of DOA estimation still standing in a wide range of applications e.g. cellular communications, radar, sonar, astronomy and military due to its outperform and practical functionality in locating emitting sources (Chen, Gokeda, & Yu, 2010). Generally, localization process may involve joint estimation of frequencies, phase shifts, DOA and TOA (Salamah & Doukhitch, n.d.). One approach called a joint estimation of DOA to rely on a time delay of the received signal. Such a process requires the transmitted signal to be known before operation (Wax & Leshem, 1996). The method may produce good performance but most of the time the type of transmitted signal is unknown.

On the DOA estimation side, researchers show great interest in calculating the most accurate value of the DOA of the signal. The researchers have presented many alternatives to the problems to reach real values for both narrowband and wideband signals (Bilgehan & Abdelbari, n.d.; Cheng, Yu, Gu, & Su, 2013; ke Nie, zheng Feng, Xie, Li, & fei Xu, 2016; Y. Wang, Yang, Chen, & Xiang, 2016). One of the problems is considered to be the low SNR value of the signal (Shi, Yang, Shi, rui Zhu, & Hu, 2017; J. Zhang, Qiu, Song, & Tang, 2014). Another point to consider is the precision of the deterministic matrix for the signal representation (J. Liu et al., 2015; Marinho et al., 2018; Wen & So, 2015). The calculation process in the DOA estimation normally uses a large number of snapshots to achieve accuracy (Vincent, Pascal, & Besson, 2017). There is a trade-off between the number of snapshots and accuracy (Liao & Fannjiang, 2016). However, increasing the number of snapshots increases the computational cost and needs some consideration (Yan, Wang, Liu, Cao, & Jin, 2018). Finally, the DOA estimation only estimates the direction from where the signal received. There are no introduction of a full locating procedure that gives the location of the sources based on the DOA estimation.

## 1.2 Scope and Contributions of The Thesis

This thesis considers the localization of multiple signals using DOA estimation from the array signal processing point of view. This thesis does not cover the hardware implementations and specification of the aforementioned systems. However, a full detailed descriptions are provided for all introduced techniques which can be used for further implementation and developments. Moreover, practical and low complexity algorithms are provided that can be used directly in real life applications. The contributions can be summarized as:

- A new localization system consists of two stages; first a spectrum sensing and edge detection of unknown sources within the frequency spectrum of interest. The second stage is a new wideband DOA estimation method. The introduced DOA estimation method is a modified version of TOPS method and called Minimum Noisy Subband-TOPS (MNS-TOPS) method. MNS-TOPS method removes the false peaks in TOPS method in low SNR and achieve lower Root Mean Square Estimate (RMSE) values than TOPS and its recent improvements.
- A novel wideband DOA estimation method based on probabilistic approaches. The new method called Probabilistic Evaluation of Subspaces Orthogonality (PESO) method. The introduced method uses Supervised Singular Value Decomposition (SupSVD) method which is an improvement of Singular Value Decomposition (SVD). The new method expresses the reference frequency subband using other frequency subbands. The introduced DOA method is superior to latest DOA estimation methods and achieves zero bias for very close sources.
- A novel narrowband DOA estimation method called Probabilistic Estimation of Several Signals (PRESS). The introduced method has been developed based on the probabilistic approach and TOPS wideband-based method for the narrowband signals. The introduced method achieves higher accuracy than recent and existing methods.
- A full DOA estimation-based localization procedure that is suitable for a set of stationary array of antenna and On-board moving surveillance vehicle e.g. Unmanned Aerial Vehicle (UAV) and Robot.

### 1.3 List of Publications

The following list of publications includes all the published research articles during my PhD program whither related to the PhD research or not.

#### *(1) List of journal articles:*

- Bilgehan, B., & Abdelbari, A. (2019). Fast detection and DOA estimation of the unknown wideband signal sources. *International Journal of Communication Systems*, 32(11), e3968. (e3968 dac.3968) doi: 10.1002/dac.3968 (Bilgehan & Abdelbari, 2019a)
- Haci, H., & Abdelbari, A. (2020). Throughput enhanced scheduling (TES) scheme for ultra-dense networks. *International Journal of Communication Systems*, 33(4), e4229. (e4229 dac.4229) doi: 10.1002/dac.4229 (Haci & Abdelbari, 2020)
- Abdelbari, A., & Bilgehan, B. (2020). A probabilistic-based approach for direction-of-arrival estimation and localization of multiple sources. *International Journal of Communication Systems*, 33(11), e4425. (e4425 dac.4425) doi: 10.1002/dac.4425 (Abdelbari & Bilgehan, 2020b)
- Abdelbari, A., & Bilgehan, B. (2021). PESO: probabilistic evaluation of subspaces orthogonality for wideband DOA estimation. *Multidimens. Syst. Signal Process.*, 32(2), 715–746. doi: 10.1007/s11045-020-00757-6 (Abdelbari & Bilgehan, 2021)

#### *(2) List of conference papers:*

- Haci, H., & Abdelbari, A. (2019). A novel scheduling scheme for ultra-dense networks. In 2019 international symposium on networks, computers and communications (ISNCC) (p. 1-6). doi: 10.1109/ISNCC.2019.8909118 (Haci & Abdelbari, 2019)
- Abdelbari, A., & Haci, H. (2019a). Fuzzy logic-based user scheduling scheme for 5G wireless networks and beyond. In International conference on theory and application of soft computing, computing with words and perceptions (pp. 429–435). (Abdelbari & Haci, 2019a)
- Bilgehan, B., & Abdelbari, A. (2019b). A novel DOA estimation method for wideband

sources based on fuzzy systems. In International conference on theory and application of soft computing, computing with words and perceptions (pp. 405–412). (Bilgehan & Abdelbari, 2019b)

- Abdelbari, A., & Hacı, H. (2019b). An opportunistic user scheduling scheme for ultra-dense wireless networks. In 2019 11th international conference on electrical and electronics engineering (ELECO) (p. 1080-1084). doi: 10.23919/ELECO47770.2019.8990469 (Abdelbari & Hacı, 2019b)
- Abdelbari, A., & Bilgehan, B. (2020a). A novel DOA estimation method of several sources for 5G networks. In 2020 international conference on electrical, communication, and computer engineering (ICECCE) (p. 1-6). doi: 10.1109/ICECCE49384.2020.9179306 (Abdelbari & Bilgehan, 2020a)
- Naser, N., & Abdelbari, A. (2020). Estimation of global solar radiation using back propagation neural network: A case study Tripoli, Libya. In 2020 international conference on electrical, communication, and computer engineering (ICECCE) (p. 1-5). doi: 10.1109/ICECCE49384.2020.9179201 (Naser & Abdelbari, 2020)

## CHAPTER 2

### NEW WIDEBAND DOA ESTIMATION TECHNIQUES

#### 2.1 Introduction

In this chapter, the basics of DOA estimation for both narrowband and wideband signals will be reviewed then the most well-known estimation methods will be previewed which applied to narrowband signals directly. Also, we will review the main idea behind these estimation methods which is the orthogonality of signal and noise subspaces.

#### 2.2 Signal Model

The model is built on the assumption of having a receiving Uniform Linear Array (ULA) with  $M$  antennas. The distance between the antenna sensors is denoted with variable  $d$ . The distance  $d$  have a requirement to be half the bandwidth of the highest received frequency. Let us now assume  $D$  far-field sources are transmitting in wideband format. The wideband signals are ergodic and stationary zero-mean Gaussian random processes using the same center frequency  $f_c$  and same bandwidth  $B$ . The signals received at the antenna sensors are assumed to be linearly independent and without correlation. The signal can be represented as:

$$x_m(t) = \sum_{k=1}^D s_k(t - u_m \sin \theta_k) + n_m(t), \quad (2.1)$$

$$x_m(t) = \sum_{k=1}^D a_m(\theta_k) \cdot s_k(t) + n_m(t), \quad (2.2)$$

where  $s_k(t)$  is the  $k$ th received independent signal. In (2.1), the signal includes a delay in time. The delay time is due to the separation between the sensors. The first sensor is taken to be the reference. The time delay is a phase shift in the frequency domain and can be represented as in (2.2). The variable  $a_m(\theta_k)$  represents the steering vector which has the estimated value for the  $k$ th signal. The steering vector has a relation with the source of the

$k$ th received wavefront impinging on the array with  $\theta_k$  angle. The  $u_m = \frac{d_m}{v}$  where  $d_m = (m-1)d$ ,  $d$  is the distance between sensors and  $v$  is the wave propagation speed (Chen et al., 2010). The signal model in (Schmidt, 1986) assumes  $D$  signals with additional noise. The additive noise  $n_m(t)$  at each array element is assumed to be ergodic, stationary zero-mean Gaussian random processes, and independent of the incident signals (Lee & Wengrovitz, 1991).

The signals in wideband the  $a_m(\theta_k)$  denotes the steering vector that depends on the frequency and not only the angle of arrival as in narrowband signals. The narrowband signal is treated as a single frequency while the wideband signal is divided into several narrowband signals. The subdivision process sampled and use Fast Fourier Transformation (FFT) to identify  $L$  frequency bins (Yoon, Kaplan, & H. McClellan, 2006). Therefore, the wideband signal model can be represented as:

$$\mathbf{X}(f_j) = \mathbf{A}(f_j, \theta_k) \mathbf{S}(f_j) + \mathbf{N}(f_j), \quad (2.3)$$

$$\mathbf{X}_m(f_j) = \sum_{k=1}^D \mathbf{S}_k(f_j) e^{-j2\pi f_j u_m \sin \theta_k} + \mathbf{N}_m(f_j), \quad (2.4)$$

where  $\mathbf{A}(f_j, \theta)$  denotes the steering matrix at the  $j$ th frequency and  $m = 1, 2, 3 \dots M$  represents the number of array elements. The variable  $\mathbf{N}_m(f_j)$  denotes the noise vector addition on each sensor at the  $j$ th frequency. The steering matrix can be represented as:

$$\mathbf{A}_m(f_j, \theta_k) = \begin{bmatrix} \mathbf{a}_1(f_j, \theta_k) & \dots & \mathbf{a}_M(f_j, \theta_k) \end{bmatrix}^T \quad (2.5)$$

$$= \begin{bmatrix} 1 & e^{-j2\pi f_j u_1 \sin \theta_k} & \dots & e^{-j2\pi f_j u_{M-1} \sin \theta_k} \end{bmatrix}^T. \quad (2.6)$$

The steering vector  $a_m(\theta_k)$  will be represented as  $\mathbf{a}_m(f_j, \theta_k)$ , and bold  $\mathbf{A}$  represents the steering matrix. The  $[M \times M]$  correlation matrix can be represented as:

$$\mathbf{C}_{xx} = E\{\mathbf{X}(f_j) \mathbf{X}^H(f_j)\} \quad (2.7)$$

$$= \mathbf{A}(f_j, \theta_k) \mathbf{S}_{ss}(f_j) \mathbf{A}^H(f_j, \theta_k) + \sigma^2(f_j) \mathbf{I}, \quad (2.8)$$

The variable  $E\{\cdot\}$  represents the statistical expectation,  $\mathbf{S}_{ss}$  denotes the signal correlation matrix,  $\sigma^2$  is the variance of the noise,  $\mathbf{A}^H$  is the Hermitian conjugate of the steering matrix, and  $\mathbf{I}$  is the identity matrix (Chen et al., 2010). The correlation matrix in such process is unknown and need to be estimated as:

$$\hat{\mathbf{C}}_{xx} = \frac{1}{N} \sum_{i=1}^N \mathbf{X}_i(f_j) \mathbf{X}_i^H(f_j), \quad (2.9)$$

The process is well explained in  $N$  snapshots (Stoica & Nehorai, 1989). The variable named  $\mathbf{C}_{xx}$  is a Hermitian matrix.

### 2.3 Conventional DOA Estimation Methods

The incoherent DOA methods use the correlation matrix of each frequency bin directly to identify the narrow bands. The average value of the correlation matrix leads to estimate the angle of the sources. The coherent methods use the transformation matrix to exploit the internal spatial information within each frequency bin (el Ouargui, Frikel, & Said, 2018). In this section, two well-known DOA methods representing both incoherent and coherent classifications are reviewed.

#### 2.3.1 IMUSIC

The Incoherent MUSIC method calculates the Eigen Value Decomposition (EVD) for each correlation matrix that identifies the  $M$  eigenvalues and corresponding eigenvectors. The highest ( $D$ ) eigenvalues and their corresponding eigenvectors represents the signal subspace. The remaining smallest eigenvalues ( $M - D$ ) and the corresponding eigenvectors represent the noise subspace of the  $j$ th frequency bin. This can be represented as:

$$\mathbf{E}_n(f_j) = [V_{D+1} \ V_{D+2} \ \cdots \ V_M], \quad (2.10)$$

where  $V$  represents the eigenvector corresponding to noise subspace. The IMUSIC algorithm applies the narrowband MUSIC method to obtain the spatial spectrum for each frequency bin. The IMUSIC spatial spectrum is calculated by

$$\mathbf{F}(\theta) = \arg \min \left\{ \frac{1}{L} \sum_{j=1}^L \mathbf{a}^H(f_j, \theta) \mathbf{E}_n(f_j) \mathbf{E}_n^H(f_j) \mathbf{a}(f_j, \theta) \right\}. \quad (2.11)$$

The detected peaks within the spatial spectrum are corresponding to the estimated DOAs (Wax, Shan, & Kailath, 1984).

In favor conditions e.g. high SNR values ( $\geq 10dB$ ), well separated sources and high number of snapshots ( $N \geq 100$ ), IMUSIC is usually effective and achieves high resolution and very low bias from the true DOAs. However, in low SNR values, which is the case in many situations, IMUSIC suffers from the noise that assumed to be flat over the frequency range, and though, it produces peaks at wrong angles (Yoon, Kaplan, & McClellan, 2006).

### 2.3.2 TOPS

The TOPS method proposed in (Yoon, Kaplan, & McClellan, 2006) that the transformation of the steering matrix at  $j$ th frequency bin to another focusing frequency called reference frequency does not change the spatial information within the transformed steering matrix. Unlike other coherent methods that apply the transformation matrix once and the transformed steering vectors corresponding to the true DOAs are altered. TOPS transformation matrix is calculated by:

$$\Psi_{m,m}(f_l, \theta_l) \mathbf{a}_m(f_j, \theta_j) = \mathbf{a}_m(f_h, \theta_h) \quad (2.12)$$

where  $f_h = f_l + f_j$ . This transforms the steering matrix from frequency  $j$ , angle  $\theta_j$  to frequency  $h$ , angle  $\theta_h$ . This is consistent with the aim of the TOPS method where all frequencies are superimposed into a single frequency bin.

Once the correlation matrices are estimated, the EVD for each frequency bin can be calculated to obtain the signal subspace  $\mathbf{E}_s(f_j)$  of the  $j$ th frequency bin. The process can be represented as:

$$\mathbf{E}_s(f_j) = [V_1 \ V_2 \ \cdots \ V_D]. \quad (2.13)$$

Since the signal subspace  $\mathbf{E}_s(f_j)$  spans the same range as the steering matrix, TOPS proposed



that the range space spanned by the transformed signal subspace is the same as of the original steering matrix  $\mathbf{A}_m(f_j, \theta)$ . This can be represented as:

$$\text{range}\{\Psi_{m,m}(\Delta f, \vartheta)\mathbf{E}_s(f_j)\} = \text{range}\{\mathbf{A}_m(f_j, \theta)\}, \quad (2.14)$$

where  $\Delta f = f_i - f_j$  and  $\Psi$  is the hypothesis search angle. At last, the TOPS method constructs the following matrix as:

$$\mathbf{Q}(\vartheta) = \begin{bmatrix} \mathbf{Y}^H(f_1)\mathbf{E}_n(f_1) & \cdots & \mathbf{Y}^H(f_L)\mathbf{E}_n(f_L) \end{bmatrix} \quad (2.15)$$

where  $\mathbf{E}_n(f_j)$  is the noise eigenvectors of the  $j$ th frequency bin and

$$\mathbf{Y}(f_j) = \mathbf{P}(f_j)\Psi_{m,m}(\Delta f_j, \vartheta)\mathbf{E}_s(f_0) \quad (2.16)$$

where  $\Delta f_j = f_j - f_0$ . However, the implementation of  $\mathbf{Q}$  matrix encounters some errors that affect the overall resolution (Hayashi & Ohtsuki, 2016). Therefore, the projection matrix  $\mathbf{P}(f_j)$  in the null space of  $\mathbf{a}_m(f_j, \vartheta)$  is used and calculated as:

$$\mathbf{P}(f_j) = \mathbf{I} - \frac{\mathbf{a}_m(f_j, \vartheta)\mathbf{a}_m^H(f_j, \vartheta)}{\mathbf{a}_m^H(f_j, \vartheta)\mathbf{a}_m(f_j, \vartheta)}. \quad (2.17)$$

Finally, spatial spectrum for the TOPS method can be represented as:

$$F(\vartheta) = \arg \min \left\{ \left( \frac{1}{l_{\min}(\vartheta)} \right) \right\} \quad (2.18)$$

where the  $l_{\min}(\vartheta)$  is the minimum singular value at each  $\vartheta$  hypothesis search angle of the  $\mathbf{Q}$  matrix in (2.15). The estimated DOA occurs when  $\mathbf{Q}$  matrix losses its rank ( $\vartheta = \theta$ ) (J. Zhang et al., 2010).

### 2.3.3 Squared-TOPS

An improvement to the TOPS method has been introduced in Squared-TOPS method to enhance the accuracy of the DOA estimation. This advantage is done in Squared-TOPS method by re-implementing the  $\mathbf{Q}$  matrix in Equation 2.15 as follows:

$$\mathbf{Q}(\vartheta) = \begin{bmatrix} \mathbf{Y}^H(f_1)\mathbf{E}_n(f_1)\mathbf{E}_n^H(f_1)\mathbf{Y}(f_1) & \mathbf{Y}^H(f_2)\mathbf{E}_n(f_2)\mathbf{E}_n^H(f_2)\mathbf{Y}(f_2) & \cdots & \mathbf{Y}^H(f_L)\mathbf{E}_n(f_L)\mathbf{E}_n^H(f_L)\mathbf{Y}(f_L) \end{bmatrix} \quad (2.19)$$

Then by applying the SVD to Equation 2.19 and taking the least singular values, the spatial spectrum is plotted.

### 2.3.4 Weighted squared TOPS

Further enhancement to the TOPS method proposed in (Hayashi & Ohtsuki, 2016) which called Weighted Squared TOPS (WS-TOPS). WS-TOPS method contributes in two points. Firstly, to reduce the false peaks in the spatial spectrum, the  $\mathbf{Q}$  matrix in Equation 2.19 is implemented as follows:

$$\mathbf{Q}(\vartheta) = \begin{bmatrix} \mathbf{Z}(f_1) & \mathbf{Z}(f_2) & \cdots & \mathbf{Z}(f_L) \end{bmatrix} \quad (2.20)$$

where

$$\mathbf{Z}(f_j) = \mathbf{Y}^H(f_j)\mathbf{E}_n(f_j)\mathbf{E}_n^H(f_j)\mathbf{Y}(f_j) + \{\mathbf{a}_m^H(f_j, \vartheta)\mathbf{E}_n(f_j)\mathbf{E}_n^H(f_j)\mathbf{a}_m(f_j, \vartheta)\} \frac{1}{M} \quad (2.21)$$

The minimum singular values of matrix  $\mathbf{Q}$  represent the estimated DOA.

Secondly, by using weighting factor in the calculations of S-TOPS spectrum as follows:

where

$$w_j = e_{s,min}/e_{n,max} \quad (2.22)$$

$e_{s,min}$  is the least eigenvalue representing signal subspace and  $e_{n,max}$  is the highest eigenvalue representing noise subspace. The weighting factor reduces the accuracy of estimation in case of noisy frequency bins, though a threshold is used to tackle this problem.

After processing Equation 2.20 and calculating the SVD for each hypothesis search angle, the spatial spectrum can be calculated by:

$$F(\theta) = \arg \max \left\{ \frac{1}{\frac{1}{K} \sum_{j=1}^L w_j l_{min}(\theta)} \right\} \quad (2.23)$$

The improvements of WS-TOPS method reduce the false peaks and enhance the resolution of the estimation. However it does not give a good solution on how to select the reference frequency. Also, the computational costs are increased compared to the original TOPS algorithm (Hayashi & Ohtsuki, 2016).

## **2.4MNS-TOPS**

The DOA estimation in TOPS algorithm requires the carrier, lower and higher frequencies for the signal under consideration. This becomes very difficult in the applications that the source of the wideband signal is not known. Typical applications may be in astronomy, unidentified signal reception or illegal broadcasting. Therefore, motivated by the desire to identify the direction of unknown wideband signal sources and to reduce the computational complexity of the TOPS-based DOA estimation method, this research has been carried out to make an improvements on the wideband signal for the DOA estimation methodology as follow:

- First, an edge detection algorithm is developed to identify the frequency spectrum of the wideband signal arriving from a specific direction. The characteristic details of the signal of interest extracted from the frequency spectrum.
- Second, the analysis stage followed by a new TOPS-based DOA estimation method. The estimation of the DOAs analyzed by measuring the orthogonal relationship between the signal and the noise subspaces of multiple frequency components of the sources. The TOPS method modified to utilize sub-band as a reference rather than the complete incoming signal spectrum.

The new contribution produced a comparable improvement to the TOPS method. The overall resolution improved as the new DOA estimation method compared with TOPS, Squared-TOPS, and WS-TOPS methods through computer simulated wideband signal. The performance analysis shows that the introduced method works better than the classical TOPS algorithm and its improvements at all levels of SNR ranges.

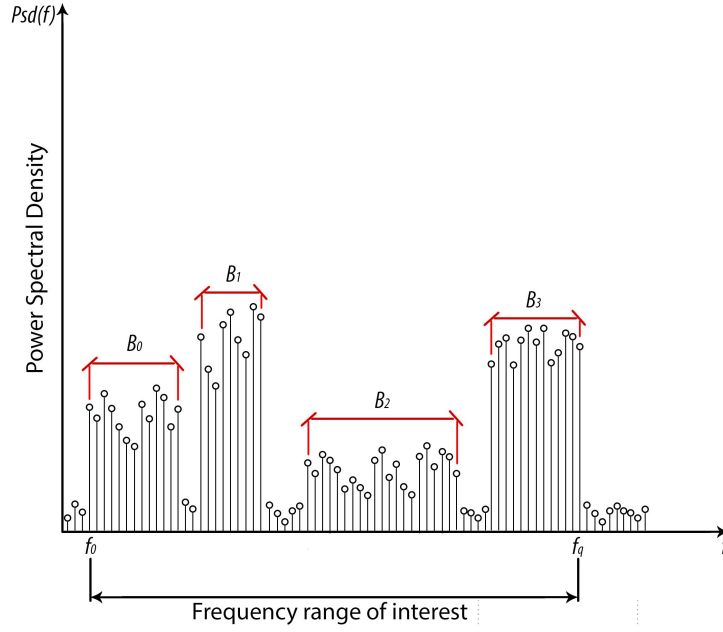


**Figure 2.1:** Visual illustration of the edge detection process.

#### 2.4.1 Signal Detection

Let's consider a wide range of frequencies of  $Q$  Hz from  $[f_0$  to  $f_q]$  which is the range of interest. Assume a  $P$  wideband signals lie within this frequency range where the number of signals, the bandwidth of each signal and the DOAs are unknown to the observer (Tian & Giannakis, 2006). The Power Spectrum Density (PSD) of those frequency wideband is assumed to be flat while its levels still unknown illustrated in Figure 2.1 (Saleem, Al-Ghathban, & Al-Naffouri, 2012).

The PSD of the incident signals is calculated by:

$$Psdf(f) = \sum_{r=1}^P \beta^2 X_r(f) + N(f), \quad (2.24)$$

where  $\beta^2$  is the signal power density and  $X_r(f)$  is the spectral form for the normalized power of each band which approximated as:

$$X_r(f) = \begin{cases} 1, & \forall f \in Q_r \\ 0, & \forall f \notin Q_r \end{cases} \quad (2.25)$$

and the  $N(f)$  is the white additive noise.

The edge detection using a multi-scale approach uses a wavelet transform of the incident signal as follows

$$T_s X_r(f) = X_r(f) * \phi_u(f), \quad (2.26)$$

where the wavelet smoothing function calculated by

$$\phi_u(f) = \frac{1}{u} \phi_u\left(\frac{f}{u}\right), \quad (2.27)$$

which could be for example a Gaussian function,  $u$  is a dilated factor and its values is set to a dyadic scale  $s = 2^i$ ,  $i = 1, 2, \dots$ , is an integer number and  $*$  denotes the convolution process. To detect the edges, the maxima of the Equation 2.26 is calculated where the first-order derivative determines it which given by

$$T'_s = |X_r(f) * \phi_u(f)|', \quad (2.28)$$

where  $T'_s$  is the first-order derivative of  $T_s X_r(f)$  (Candes, Romberg, & Tao, 2006). The frequency edge value can be calculated as

$$\hat{f}_r = \max\{T'_s\}, \quad (2.29)$$

where  $\hat{f}_r$  is the  $r$ th estimated edges. This estimated edges is used to determine the signals and calculate its bandwidth as follows:

$$\hat{B}_r = \hat{f}_r - \hat{f}_{r-1}, \quad (2.30)$$

and the center frequency is  $f_{c,r} = (\hat{f}_r + \hat{f}_{r-1})/2$ . Using a band pass filter e.g. Hilbert or Butterworth to extract the  $r$ th signal of interest for further estimation of its DOA(Lv & Liu, 2013).

### 2.4.2 Proposed methodology

The reference frequency  $f_0$  is a significant factor in the TOPS method. The selection of the reference frequency as the highest difference between  $e_{s,min}$ , the least eigenvalue corresponding to signals, and  $e_{n,max}$ , the highest eigenvalue corresponding to noises, produces the highest resolution by selecting lowest interference with noise as:

$$f_0 = \max\{e_{s,min} - e_{n,max}\}. \quad (2.31)$$

Also, TOPS method is very complex due to the calculation of eigen decomposition for all frequency bins. The calculation of the transformation matrix adds more computational costs (Yoon, 2004). Therefore, in this research, a new method for the calculation of the reference frequency is proposed. For  $L$  frequency bins within the wideband signal, the reference frequency calculated as the minimum absolute integer as:

$$f_{0,new} = \min \left| \frac{L}{f_s} \cdot \text{mod}\left(\frac{f_c}{f}\right) - d \right| \quad (2.32)$$

where  $\text{mod}(\cdot)$  is the reminder function and  $f_s$ ,  $f_c$  and  $d$  the sampling frequency, the center frequency and the array elements displacement, respectively. This introduced method produces less computational cost and achieves higher resolution than conventional TOPS methods.

Based on the idea of using spatial information of all frequency bins and different frequency bins have better spatial information than others, another improvement could be made to improve the accuracy of the algorithm. This work proposes to calculate the SVD for every  $\mathbf{Z}(f_j)$  matrix in equation 2.21 rather than using a weight factor for every hypothesis search angle after the transformation of all frequency bins into the reference frequency. The process follows with the summation of all minimum singular values for all frequency bins. The process can be expressed as:

$$F(\theta) = \arg \max \left\{ \sum_{j=1}^L l_{Z,min}(\theta) \right\} \quad (2.33)$$

The ratio in Equation 2.22 identifies the valuable frequency bins. A threshold technique

applied to use only the valuable frequency bins that have better spatial information and are less affected by noise.

$$w_j = e_{s,min}/e_{n,max} \geq w_{th} \quad (2.34)$$

where  $w_{th}$  is a threshold value.

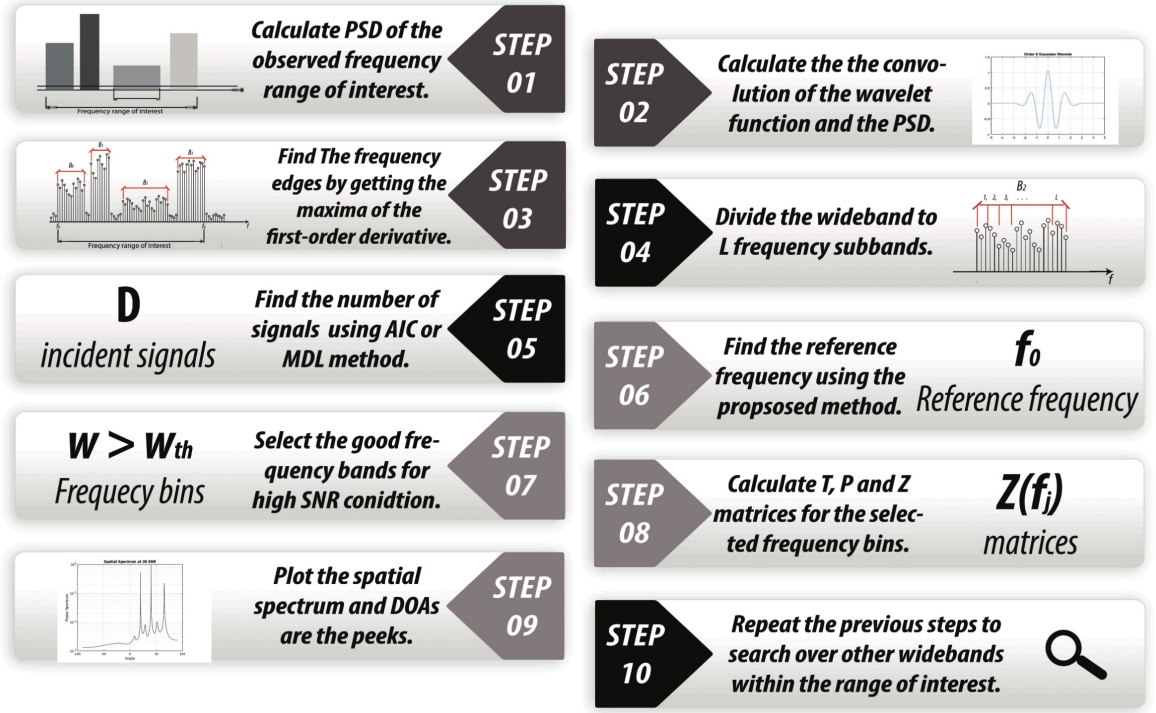


**Figure 2.2:** The proposed algorithm.

This reduces the number of frequency bins  $L$  applying to the algorithm. The process disregards the rest of the frequency bins from the algorithm execution. The selection of the threshold value  $w_{th}$  of the frequency bin selective indicator depends on the gap between the signal and noise subspaces. The proposed method uses the mean values of all selective indicator formulated as:

$$w_{th} = \frac{1}{L} \sum_{j=1}^L w_j(\theta) \quad (2.35)$$

The equation 2.35 applied successfully to both low and high values of the SNRs. Both of which demonstrate different characteristics. The computational difference between each

round of the signal and noise subspace calculation varies drastically. The wideband signal with high SNR produce large difference between computational points whereas the frequency bins are highly effected by noise and the separation between the computational points becomes very small at the low SNR. Finally the selective TOPS spatial spectrum is represented as:

$$F(\theta) = \arg \max \left\{ \frac{1}{\sum_{j=1}^B l_{Z,min}(\theta)} \right\}, \quad (2.36)$$

where the number of selected frequency bins  $B$  is calculated as:

$$B = \begin{cases} L, & \forall SNR < 10 \text{ dB} \\ < L, & \forall SNR \geq 10 \text{ dB} \end{cases} \quad (2.37)$$

The selected value of SNR is based on numerical calculation and can be varied accordingly.

In this research, an algorithm of detecting unknown signals within a frequency range of interest and estimate its location is proposed shown in Figure 2.2. The detailed version of the algorithm with relevant references is to follow.

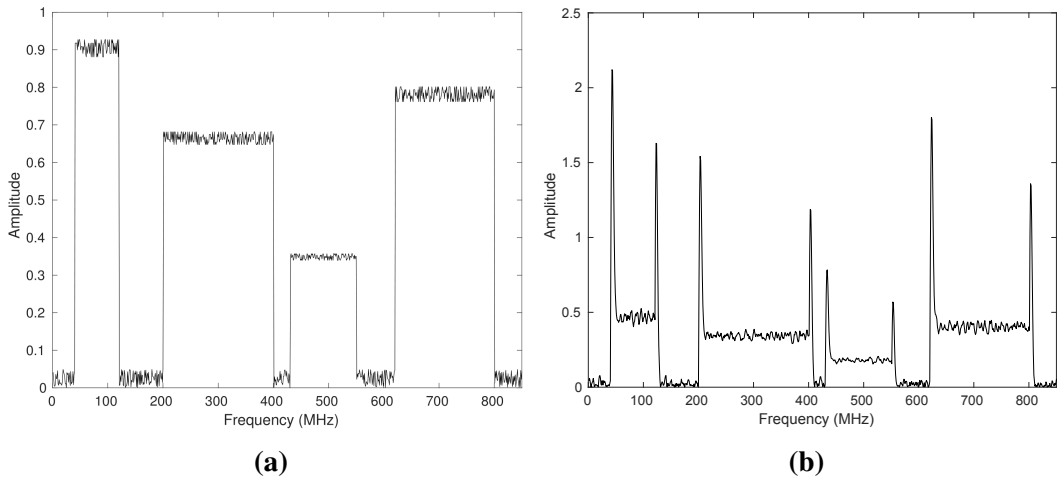


**Figure 2.3:** Edge detection stage (a) shows the frequency spectrum of interest and (b) shows the output of the edge detection.

- **Step 1:** The PSD of the incident signals is calculated by Equation 2.24.
- **Step 2:** The convolution of the wavelet function and the PSD is calculated by Equation



2.26.

- **Step 3:** The frequency edges are found by getting the maxima of the first-order derivative as in Equation 2.29 and the bandwidth is calculated by Equation 2.30.
- **Step 4:** FFT is applied and the selected wideband is divided to  $L$  frequency subbands.
- **Step 5:** Using Akaike Information Criterion (AIC) or Minimum Description Length (MDL) methods, the number of signals can be estimated.
- **Step 6:** Using the proposed method, reference frequency can be selected by Equation 2.32.
- **Step 7:** Using the selective indicator in Equation 2.34, only the good subbands will be selected.
- **Step 8:** Further, the  $\mathbf{Z}(f_j)$  matrices are calculated using Equation 2.21 for the selected frequency bins.
- **Step 9:** The DOAs of all signals can be estimated by Equation 2.33 for the minimum singular values for every hypothesis search angle.
- **Step 10:** Repeat the previous steps to search over other wideband within the range of interest.

**Table 2.1:** Simulation cases.

Simulation Case	1st Case	2nd Case	3rd Case	4th Case
Number of sensors $M$	10	8	10	10
Number of received signals $D$	3	3	3	5
Number of frequency bins $L$	26	26	16	26

### 2.4.3 Simulation results

To demonstrate the performance of the introduced DOA estimation method, a Monte Carlo simulation has been conducted on MATLAB environment for 200 trials. It is assumed that a ULA with the number of elements  $M = 10$  received within the spectrum of interest a 4 wideband signals with characteristics e.g. different center frequencies and bandwidths. One of these wideband includes a  $D = 3$  signals impinging on the ULA from a far-field at  $20^\circ$ ,

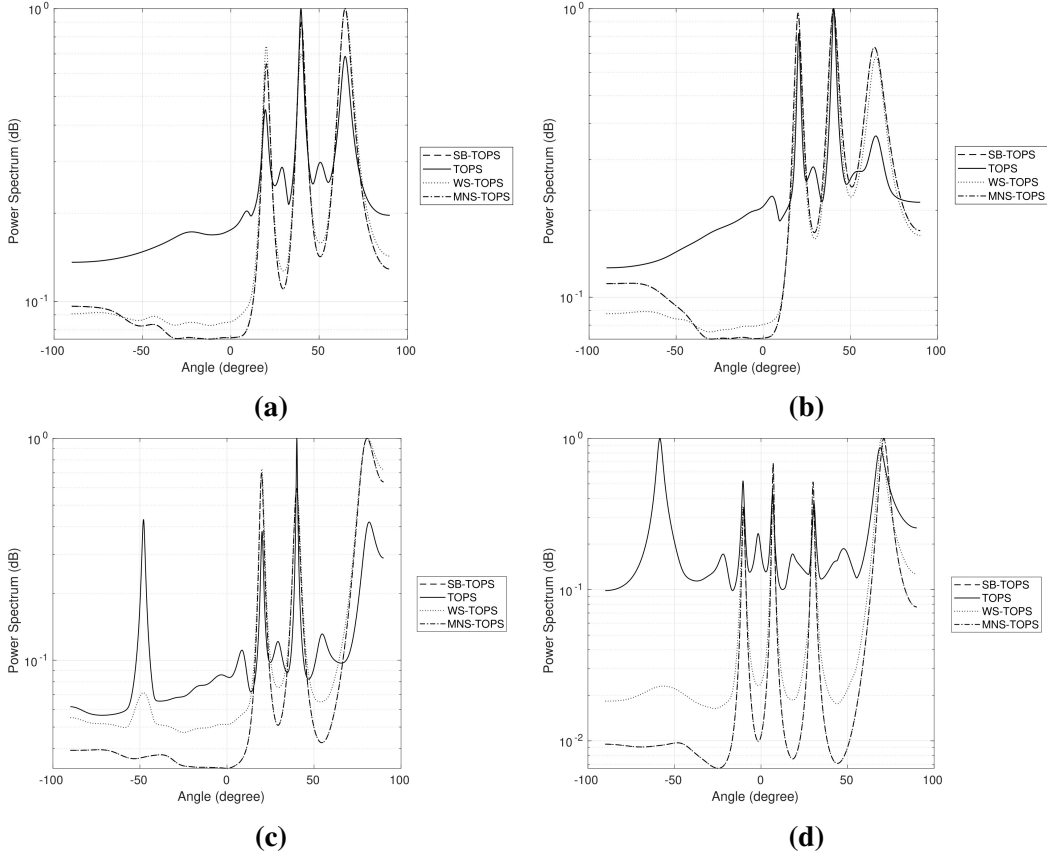


**Figure 2.4:** Spatial spectrum at SNR = -5 dB for the four simulation cases, where (a)  $M = 10, D = 3$  at  $(20^\circ \ 40^\circ \ 65^\circ)$  and  $L = 26$ ; (b)  $M = 8, D = 3$  at  $(20^\circ \ 40^\circ \ 65^\circ)$  and  $L = 26$ ; (c)  $M = 10, D = 3$  at  $(20^\circ \ 40^\circ \ 80^\circ)$  and  $L = 16$ ; and (d)  $M = 10, D = 5$  at  $(-10^\circ \ 7^\circ \ 30^\circ \ 65^\circ \ 80^\circ)$  and  $L = 26$ .

$40^\circ$  and  $65^\circ$ . These signals of interests have the same characteristics.  $f_0 = 300$ ,  $f_l = 200$ ,  $f_h = 400$ ,  $f_s = 1000$ , and  $bw = 200$  are the center frequency, lower frequency, higher frequency, Nyquist sampling frequency, and bandwidth respectively. All measured in MHz and normalized to the center frequency. The number of frequency bins is assumed to be  $L = 26$ . The signal with noise can be represented as:

$$s_i(t) = \sum_{j=1}^L g_i(t) \exp(j2\pi f_j t) + n_i(t), \quad (2.38)$$

where  $g_i(t)$  denotes the magnitude of the signal and  $n_i(t)$  denotes the Additive White Gaussian Noise (AWGN). Both are a Gaussian random variables where the signal to noise ratio is 10. The snapshots are only 20 for 128 FFT points while in the literature they used at least 100 snapshots for 256 FFT points (Yoon, Kaplan, & McClellan, 2006; Hayashi & Ohtsuki,

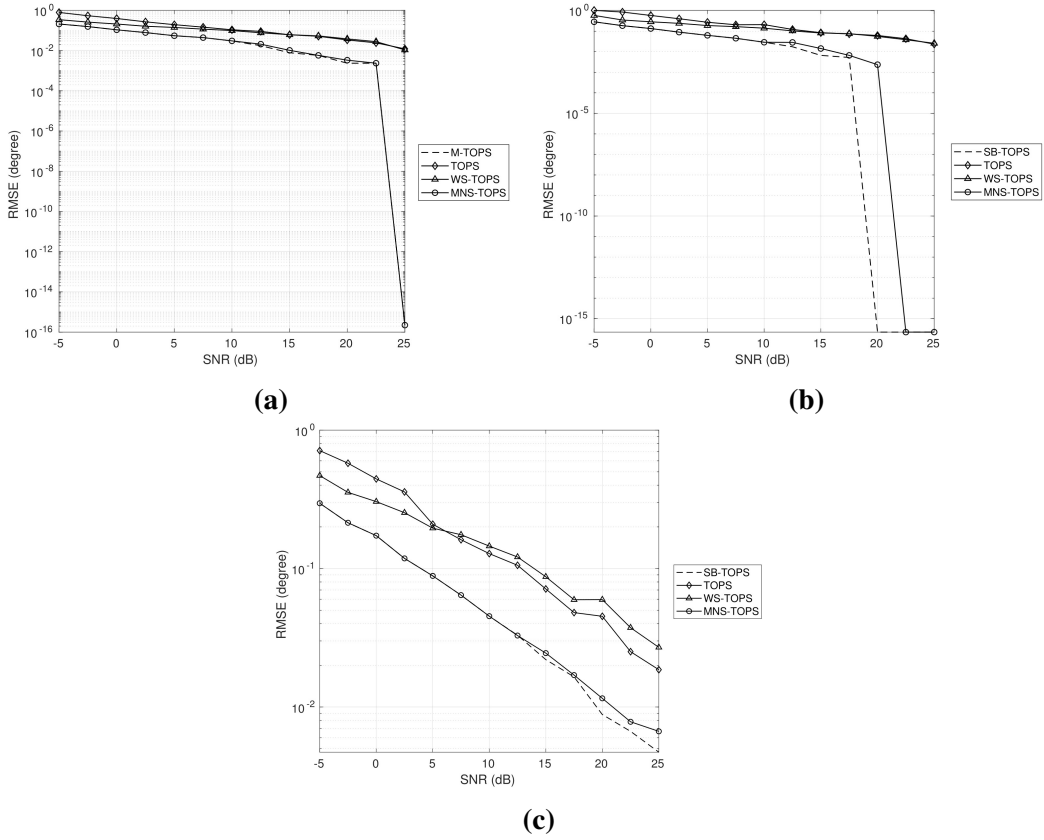


**Figure 2.5:** RMSE of all three estimated sources for the three simulation cases, where (a)  $M = 10, D = 3$  at  $(20^\circ \ 40^\circ \ 65^\circ)$  and  $L = 26$ ; (b)  $M = 8, D = 3$  at  $(20^\circ \ 40^\circ \ 65^\circ)$  and  $L = 26$ ; and (c)  $M = 10, D = 3$  at  $(20^\circ \ 40^\circ \ 80^\circ)$  and  $L = 16$ .

2016). This advantage reduces the complicity significantly. For a full test of the introduced method, 4 simulation cases have been conducted with the specifications summarized in Table 2.1. For the 1st, 2nd, and 3rd cases, the  $D = 3$  at  $(20^\circ \ 40^\circ \ 80^\circ)$ . For the 4th case tested  $D = 5$  at  $(-10^\circ, \ 7^\circ, \ 30^\circ, \ 65^\circ, \ 80^\circ)$ . The proposed method named subbands-based TOPS (SB-TOPS) uses all the frequency bins while the proposed method MNS-TOPS uses the selected frequency bins. This is just to show the effect of the improvement on the accuracy of estimation.

Figure 2.3a shows the 4 wideband signals within the frequency spectrum. It shows different power and bandwidth levels for each signal. After applying the edge detection stage, the edges clearly visible and can be detected as seen in Figure 2.3b. A peak detection algorithm can be easily applied to determine all the lower and higher frequencies of all wideband signals.

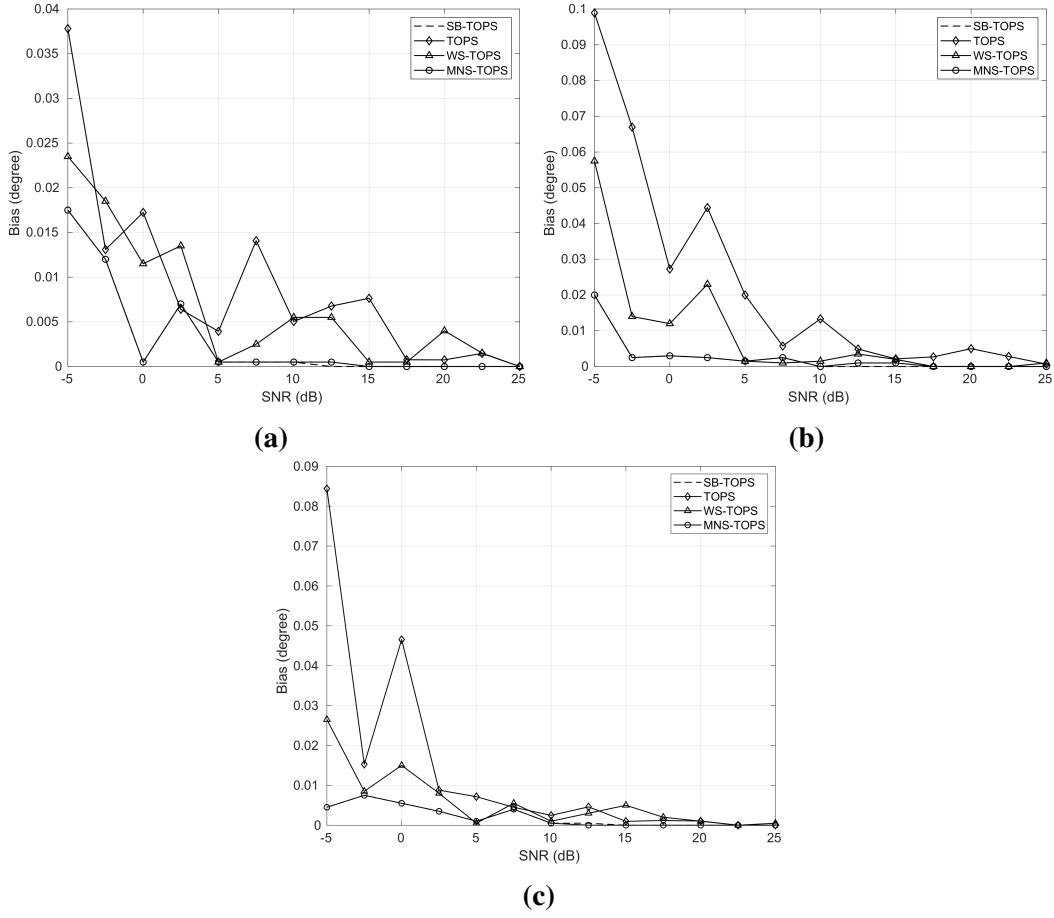


**Figure 2.6:** Bias of the first source at  $20^\circ$  for the three simulation cases, where (a)  $M = 10, D = 3$  at  $(20^\circ \ 40^\circ \ 65^\circ)$  and  $L = 26$ ; (b)  $M = 8, D = 3$  at  $(20^\circ \ 40^\circ \ 65^\circ)$  and  $L = 26$ ; and (c)  $M = 10, D = 3$  at  $(20^\circ \ 40^\circ \ 80^\circ)$  and  $L = 16$ .

Figure 2.4 shows the spatial spectrum of the proposed method compared with TOPS and WS-TOPS methods where the high peaks refer to the DOAs and false peaks. The figures are for the 4 simulation cases and measured at SNR =  $-5$  dB. For the first 3 cases, all the compared methods estimate all the correct DOAs except for TOPS method which shows peaks at the wrong angles. The proposed methods and WS-TOPS do not show such false peaks. The proposed methods record higher power level than other methods with higher resolution. In the 4th case, all methods did not estimate the DOAs at  $65^\circ, 80^\circ$  because the existence of high noise.

Figure 2.5 show the RMSE for the first 3 cases of the simulation. Generally, RMSE is calculated for the estimated DOAs of all sources by:

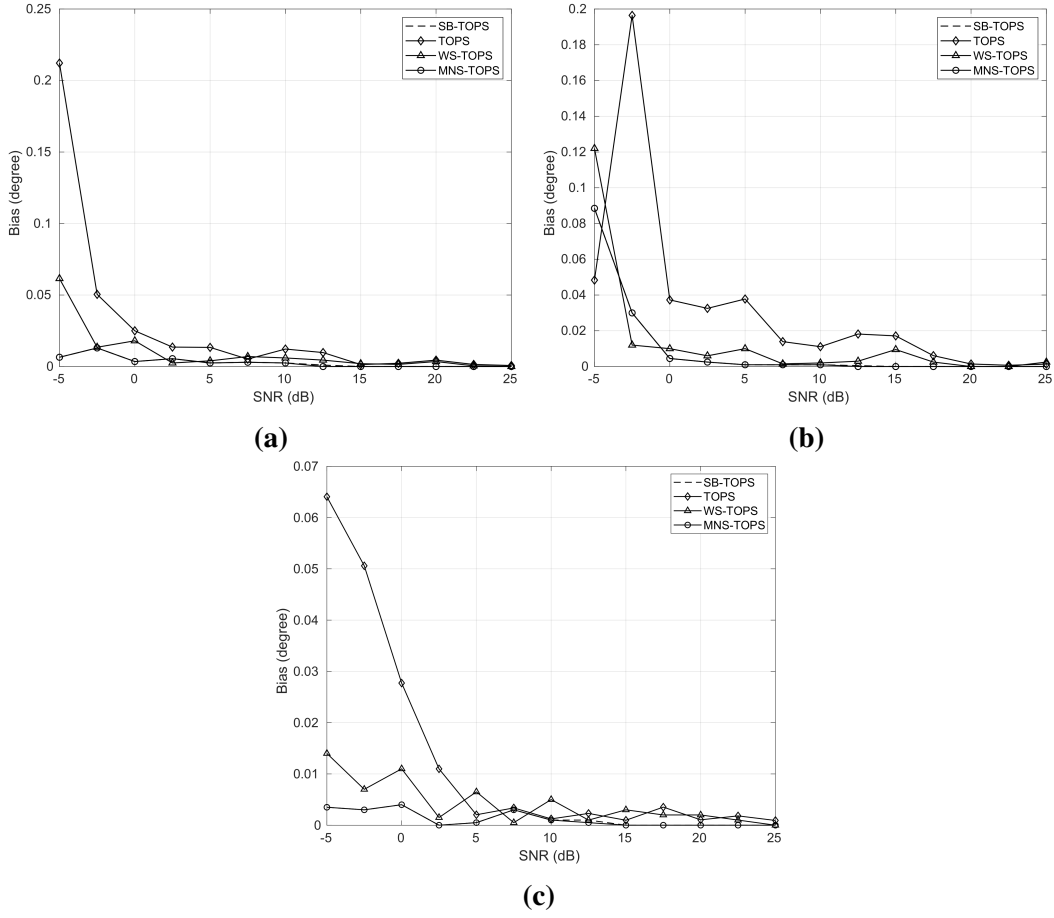


**Figure 2.7:** Bias of the second source at  $40^\circ$  for the three simulation cases, where (a)  $M = 10, D = 3$  at  $(20^\circ \ 40^\circ \ 65^\circ)$  and  $L = 26$ ; (b)  $M = 8, D = 3$  at  $(20^\circ \ 40^\circ \ 65^\circ)$  and  $L = 26$ ; and (c)  $M = 10, D = 3$  at  $(20^\circ \ 40^\circ \ 80^\circ)$  and  $L = 16$ .

$$\text{RMSE} = \frac{1}{D} \sum_{i=1}^D \sqrt{\frac{1}{200} \sum_{r=1}^{200} |\theta_i - \hat{\theta}_{i,r}|^2}, \quad (2.39)$$

where  $\theta_i$  is the  $i$ th true DOA and  $\hat{\theta}_{i,r}$  is the  $i$ th estimated DOA angle at the  $r$ th simulation round. It shows that the proposed method overcome other methods in all simulation cases. Further the the proposed methods achieve zero bias at high SNR value. Also, the use of the good frequency bins enhance the estimation which shown in the performance of the MNS-TOPS over the performance of SB-TOPS.

Figures 2.6 and 2.7 show the bias of the estimation from the actual DOA measured in degrees for the 1st and 2nd sources at  $20^\circ$  and  $40^\circ$ , respectively. The proposed methods achieve higher accuracy or less bias ( $< 0.01^\circ$ ) than other methods. With lower computational costs

**Table 2.2:** The complexity of common mathematical multiplications and stages used within DOA algorithms.

Stage	Complexity
FFT Subband extraction	$T \cdot \log(T)$
Correlation matrix	$L \cdot N \cdot O(M^2)$
EVD	$O(M^3)$
SVD	$O(M^3)$
Matrix multiplication	$O(mnp)$

due to using less number of frequency bins, the proposed method MNS-TOPS overcome SB-TOPS method at all SNR levels. This achievement without any existence of wrong estimation.

Figure 2.8 shows the execution time consumed by each method using the same machine to compare the performance of computation practically. It shows that the MNS-TOPS performance overcome other compared methods WS-TOPS and SB-TOPS which uses less number of frequency bins. In table 2.2, the common stages that most DOA estimation methods encounter. The proposed method SB-TOPS goes through the same stages as WS-TOPS method except that WS-TOPS calculates SVD once while SB-TOPS calculates SVD for each frequency bin. MNS-TOPS reduces that by selecting a subset of frequency bins. Then, by applying all the stages from beginning to only the selected frequency bins. This reduces the complexity and explain the less consumed time shown in Figure 2.8. Figure 2.9 shows the selective indicator that used by MNS-TOPS algorithm to select the frequency bins for further analysis and discard the rest. It shows that for the 3rd case where less number of frequency bins are used, higher values of the selective indicator than other cases indicates the effect of choosing number of frequency bins on the DOA estimation.

#### 2.4.4 Conclusion

The proposed method includes two practical stages to address the wideband DOA estimation of unknown sources which are target extraction and DOA estimation. Practically a mixed signals with the same bandwidth received from different locations. Therefore, an edge detection method proposed as a separation method to identifies the frequency spectrum and its characteristics. Also, the DOA estimation methods suffer from wrong estimations and low

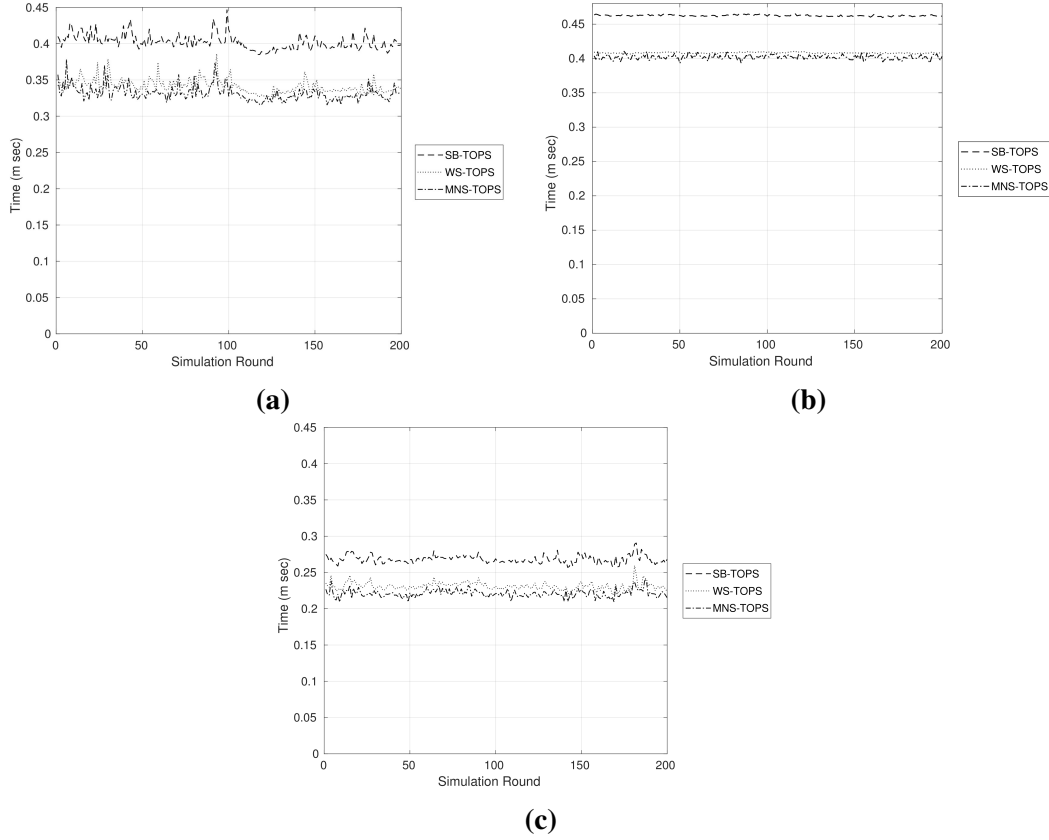


**Figure 2.8:** Mean execution time elapsed by each simulation cases, where (a)  $M = 10, D = 3$  at  $(20^\circ \ 40^\circ \ 65^\circ)$  and  $L = 26$ ; (b)  $M = 8, D = 3$  at  $(20^\circ \ 40^\circ \ 65^\circ)$  and  $L = 26$ ; and (c)  $M = 10, D = 3$  at  $(20^\circ \ 40^\circ \ 80^\circ)$  and  $L = 16$ .

accuracy (higher bias). Thus, a proposed DOA estimation algorithm uses the characteristics of the frequency bins of the targeted wideband signal to effectively determine the reference frequency. It is also use a selective indicator to select a subset of the frequency bins to reduce computational cost while sustaining a high resolution estimation. In a comparison against TOPS and WS-TOPS methods, the simulation results shows the significant performance of the introduced method.

The aims of any localization algorithm is to localize multiple targets accurately to a certain level with the minimum complexity. This is to overcome the issue of tracking each target separately which consume resources dramatically as the number of targets increase. Another issue is the time consumed to locate the targets can be repeated continuously in case of moving targets to track their movements. The localization algorithm should be at low latency to be effective and practical. In the next research work, we tried to approach that aim.

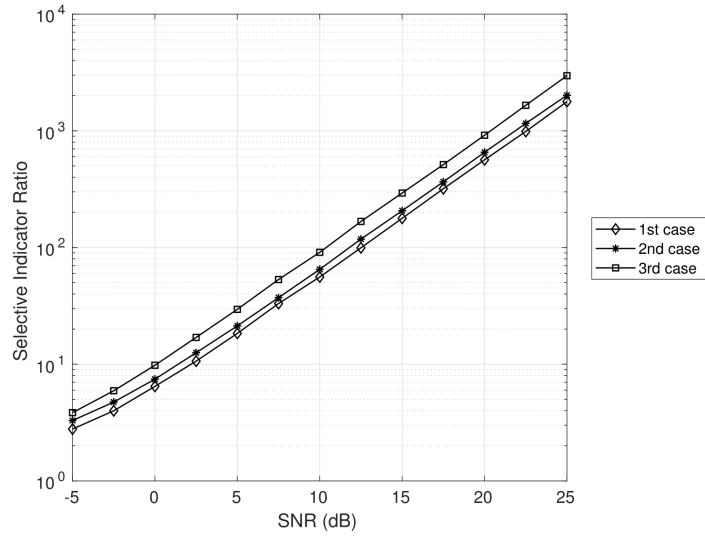


**Figure 2.9:** The selective indicator of all three estimated sources for the three simulation cases, where 1st case:  $M = 10, D = 3$  at  $(20^\circ \ 40^\circ \ 65^\circ)$  and  $L = 26$ ; 2nd case:  $M = 8, D = 3$  at  $(20^\circ \ 40^\circ \ 65^\circ)$  and  $L = 26$ ; and 3rd case:  $M = 10, D = 3$  at  $(20^\circ \ 40^\circ \ 80^\circ)$  and  $L = 16$ .

## 2.5 PESO

### 2.5.1 Introduction

In this research, we propose a new DOA estimation method for wideband signals to overcome the problems encountered so far and produce accurate estimation at the lowest values of SNRs with the least possible bias by evaluating the highest probability relation between the signal and the noise subspaces of multiple frequency components of the sources. The statistical probability of resolution in various frequency bins shows the advantage of a very low computational cost than any existing DOA estimation method. The newly introduced method uses enough frequency bins to resolve very close sources with minimum bias. The method produces a very close estimation for the transmitting sources. The new method uses a low number of snapshots for the first time. The main contribution can be classified as:

- Introducing a new DOA estimation method based on a probabilistic approach that resolves the accurate DOA with zero bias at high SNR values and resolves the DOA with the least possible bias at low SNR values.
- The statistical investigation of the probability of resolution in various frequency bins



shows an advantage which lead to reduce computational cost than any existing DOA estimation method. This enhancement can be applied to any existing DOA estimation method to increase the accuracy.

The performance of the introduced method compared with well-known methods such as IMUSIC and TOPS. The simulations show that the new technique performs better than others in all range of SNR values. The newly introduced method tested with the lowest ever used number of snapshots (30) and very low SNR values. The new method estimates the exact DOA at a lowest computational cost while the conventional methods can not produce accurate results.

### 2.5.2 The Proposed method

The proposed method introduces the idea of selecting valuable subbands for further processing while benefit from other subbands as well. The selection depends on the probability of source detection. The proposed method allows to determine an accurate DOA at high SNR values. The new method also produces the least bias at the extreme SNR values. Moreover, the proposed method studies the spatial spectrum itself without any modification to the applied narrowband DOA method.

#### (1) *Probability of source detection*

The proposed method applies to the ordinary narrowband MUSIC method for each frequency bin and obtains the spatial spectrum individually. The narrowband MUSIC spatial spectrum for the  $j$ th frequency bin can be calculated as:

$$\mathbf{F}(f_j, \phi) = \arg \min \{ \mathbf{a}^H(f_j, \phi) \mathbf{E}_n(f_j) \mathbf{E}_n^H(f_j) \mathbf{a}(f_j, \phi) \}. \quad (2.40)$$

where  $\theta$  is the hypothesis search angle  $[-90^\circ : 0.1^\circ : 90^\circ]$ .

Ideally, each frequency bin has the same spatial information before applying noise on each sensor. However, the frequencies are affected due to channel path loss variations where the signal follows a Gaussian distribution and the noise added at each sensor is an AWGN type. Therefore, some of the frequency bins are less affected by path loss and noise than others (Wax et al., 1984), and hence, the less affected frequencies are likely to contain more accurate

values of the DOA information. Moreover, because each covariance matrix is estimated using (3.5), the orthogonality between the steering vector corresponding to the DOA and the eigenvectors of the noise subspace is not ideal and accordingly, not identical from one frequency bin to another (Sharman, Durrani, Wax, & Kailath, 1984). As a result, false peaks are detected in some frequency bins' spatial spectrum and some also show only peaks corresponding to the estimated DOAs.

Let  $\mathfrak{R}_j$  be a set of detected peaks at the  $j$ th frequency bin given by

$$\mathfrak{R}_j = \{p_1, p_i, \dots, p_\beta\}, \quad \text{where } i = 1, 2, \dots, \beta \quad (2.41)$$

where  $\beta$  denotes the number of detected peaks at the  $j$ th frequency bin. To calculate the repetition of, a Mean Shifted Clustering (MSC) algorithm is proceeded (Carreira-Perpiñán, 2015). This led to a set of new angle clusters including the estimated DOAs represented by:

$$\Gamma_\varphi = \{\mathfrak{R}_1 \mathfrak{R}_2 \dots \mathfrak{R}_\varphi \dots \mathfrak{R}_R\}, \quad (2.42)$$

where  $\theta_{avg}(\mathfrak{R}_\varphi)$  is the mean angle of the  $\varphi$ th angle cluster. Beginning with any arbitrary  $j$ th frequency bin, let the distance between any two successive observed peaks to be  $l_i$ . Then the mean limit can be calculated:

$$l_i(f_j) = \frac{p_i + p_{i+1}}{2}. \quad (2.43)$$

Let a predefined search angle limit  $\Theta$  be a small positive number that can be applied around the mean angle of the  $\varphi$ th angle cluster. The peak detection method can be classified as follow. For any arbitrary detected peak  $p \in \mathfrak{R}_j$ , if  $p$  lies in-between  $\theta_{avg}(\mathfrak{R}_\varphi) - \Theta$  and  $\theta_{avg}(\mathfrak{R}_\varphi) + \Theta$ , then  $p \in \mathfrak{R}_\varphi$ .

As a result, there will be more clusters than usual. However, narrowing the band around the sources DOA will enhance the accuracy and raise the probability of the well detected peaks. The peaks occur within right angle clusters. Such processing reduces the possibility of false peaks. The false peaks often produce difficulty on both visual and mathematical estimation

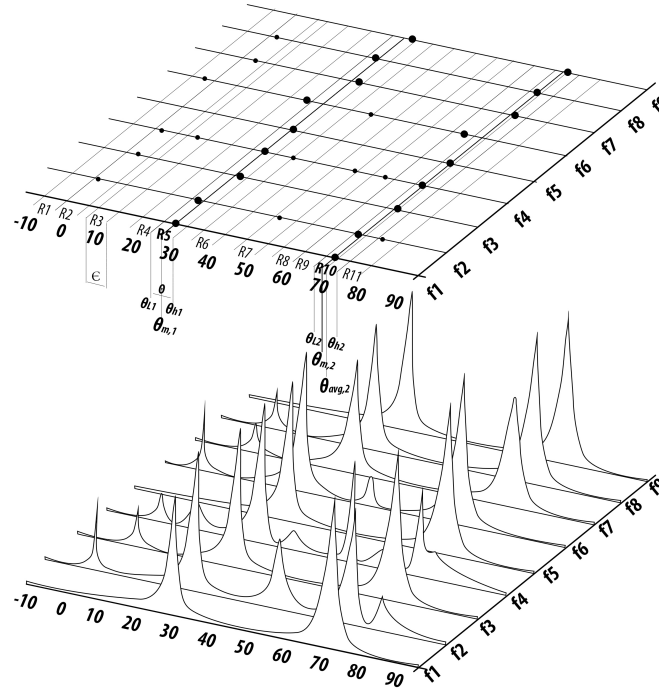


**Figure 2.10:** Visual illustration of the probability of detected peaks within the spatial spectrum of all frequency bins.

of the DOA. Fig. 2.10 visually illustrates the angle clusters that is a significant advantage in the detection of the highest probability of peaks related to the accurate DOA angles while discarding irrelevant peaks. Both, pure noises and noisy signal peaks yield high bias that makes the peak to take place outside the angle clusters  $R5$  and  $R10$ .

## (2) Determination of accurate DOA

The process of taking the average value of the spatial spectrum of all frequency bins or implementing a universal spectrum after transforming all frequency bins to a specified reference fails to detect the exact location. Moreover, it occasionally shows peaks in wrong angles at extreme conditions (Yoon, Kaplan, & McClellan, 2006). The unknown Gaussian sources produce peaks to be detected that can be represented as a random variable. (Sharman et al., 1984). Therefore, a clustering algorithm using mean shift scheme can be applied. Let the detected peaks at the  $\varphi$ th  $\mathfrak{R}_\varphi$  to be random Gaussian variables and the probability of occurrence within the  $\varphi$ th angle cluster be  $P(\mathfrak{R}_\varphi|p)$ . It is assumed that the minimum eigenvalues of noise subspace to be repeated and equal to zero

$$\lambda_{D+1} \geq \lambda_{D+2} \geq \dots \geq \lambda_M \geq 0, \quad (2.44)$$

However, in practice, they are non-zero, small values and lie within a cluster. This concludes that, there are a chance for the detected peak to be noise (Schmidt, 1986). Accordingly, the probability of occurrence  $\epsilon_\varphi(p)$  of a pure random variable representing noise is independent from source and vary with both path loss randomly and SNR gradually. Then,

$$P(\mathfrak{R}_\varphi|p) = P(\mathfrak{R}_\varphi|\theta) + \epsilon_\varphi(p), \quad (2.45)$$

where  $P(\mathfrak{R}_\varphi|\theta)$  is the probability of occurrence of the  $i$ th estimated DOA.

The probability of repetition within the  $\varphi$ th angle cluster is calculated by:

$$v_\varphi(p) = \frac{r}{\beta} \quad (2.46)$$

where  $r$  is the number of the peaks at the same angle and  $\beta$  is the total number of peaks in the  $\varphi$ th angle cluster where  $(r \leq \beta \leq L)$ . The number of occurrence  $\beta$  depends on the SNR condition and the value of  $\Theta_i$ . It has been observed that the probability of repetition of accurate DOAs is higher than the biased DOAs within the same narrow angle band where:

$$v_\varphi\{\theta_1\} \geq v_\varphi\{\theta_2\} \geq \dots \geq v_\varphi\{\theta_\beta\} \quad (2.47)$$

Hence, the accurate DOA is the one that achieve the highest probability of repetition within the  $\varphi$ th angle cluster. Other peaks within the cluster are considered as biased DOA due to the higher effect of noise. The visual examination of Fig. 2.10 highlights this lemmas where two DOA 1 and 2 are detected. While  $\theta_{m,1}$  and  $\theta_{m,2}$  are the accurate DOAs, the  $\theta_{avg,2}$  suffers from a bias. This illustrates that in some cases the total average is biased due to some frequency bins biased estimation.

The assumption in (2.47) basically depends on the SNR condition and the distance from the successive source of the DOA. Thus, in very low SNR, the probability of repetition  $v_\varphi\{\theta_i\}$  is very low and have a bias due to the inability of accurate DOA determination. The proposed method suggests to use a universal average between the cluster angles including the highest

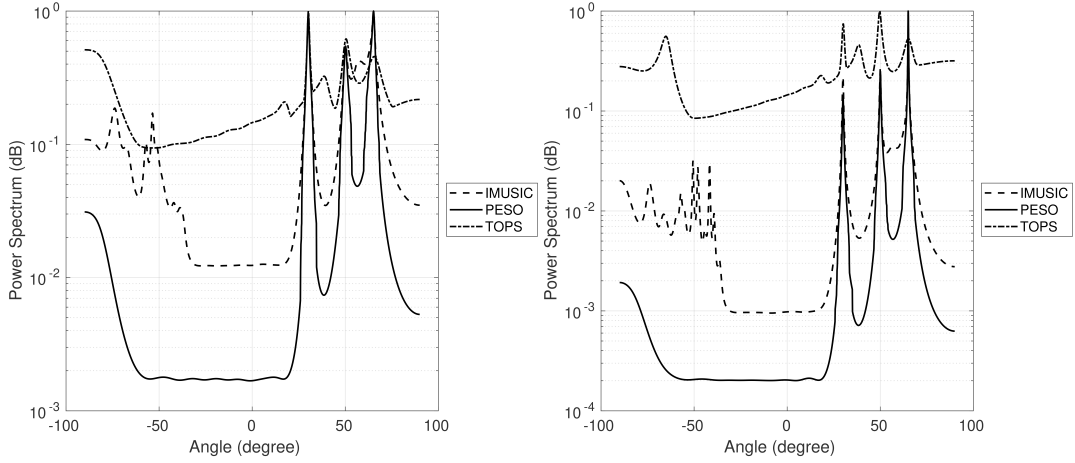


**Figure 2.11:** Normalized spatial spectrum at (a) -5 dB, and (b) -2.5 dB SNR for PESO compared with IMUSIC and TOPS methods for sources at  $30^\circ$ ,  $50^\circ$  and  $65^\circ$ .

probably estimated angle and the most least bias for the DOA will be:

$$\hat{\theta}_{Tavg} = avg\{\theta_i \pm \Theta\} \text{ where } \theta_i \in \mathfrak{R}_\varphi. \quad (2.48)$$

The clusters with the highest number of peaks occurring among the frequency bins is corresponding to the estimated DOAs. Other clusters are assumed to be noise and will be discarded. Besides, the elimination of the noise peaks, the computational cost degraded eventually. For the favor conditions ( $SNR \geq 10\text{dB}$ ), the algorithm of determining the exact DOA is processed by summing only the portions of the spatial spectrum with the exact location only. The rest of the spatial spectrum will be minimized to the lowest value in each spectrum.

$$\mathbf{F}(\phi) = \begin{cases} \frac{1}{\beta} \sum_{j=1}^{\beta} \mathbf{F}(f_j, \phi), & \text{where } \phi \in \{\theta_i \pm \Theta\} : \theta_i \in \mathfrak{R}_i \\ \frac{1}{L} \sum_{j=1}^L \min\{\mathbf{F}(f_j, \phi)\}, & \text{where } \phi \notin \{\theta_i \pm \Theta\} \end{cases} \quad (2.49)$$

where  $\mathfrak{R}_i$  is the angle cluster of the  $i$ th estimated DOA and the  $\theta_i \pm \Theta$  is the estimated DOA and surrounded angles to be clear at the visual detect of the final spatial spectrum.

The algorithmic summary of the new method:

- **Step 1:** FFT is applied to the wideband and subdivided into  $L$  frequency bins.

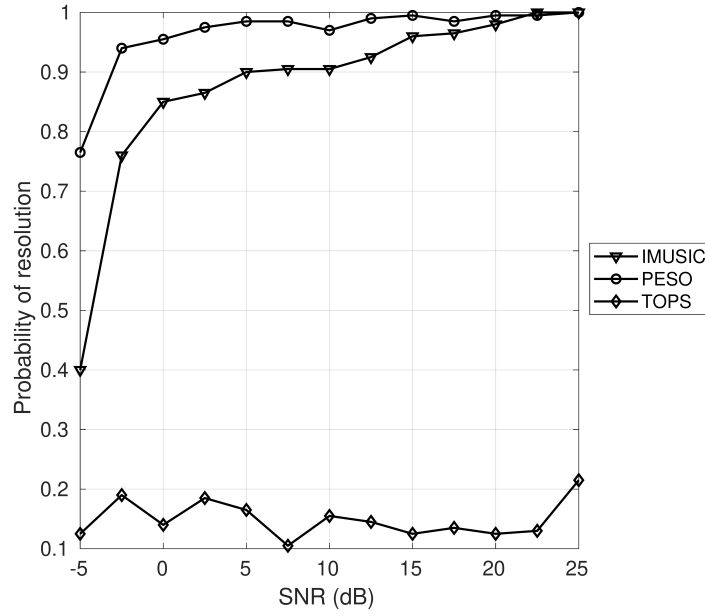


**Figure 2.12:** The probability of resolution for proposed method PESO compared with IMUSIC and TOPS methods.

- **Step 2:** Using (2.40), the spatial spectrum of each frequency bin obtained.
- **Step 3:** Apply a mean shift to arrange the observed peaks into angle clusters.
- **Step 4:** Calculate the probability of occurrence for each angle cluster.
- **Step 5:** Choose clusters with the highest probability as the DOA and discard other clusters.
- **Step 6:** Plot the final spatial spectrum using (2.49).

### 2.5.3 Simulation results

The newly proposed PESO algorithm tested using the MATLAB software for 200 Monte Carlo simulation trials. The simulation scenario includes 3 wideband sources located at positions  $30^\circ$ ,  $50^\circ$  and  $65^\circ$ . The known pre-set values are  $f_l = 200$ ,  $f_h = 400$ ,  $f_0 = 300$  and  $f_s = 1000$  MHz; the lowest frequency, the highest frequency, the center frequency, and the Nyquist sampling frequency, respectively. The bandwidth is  $bw = f_h - f_l = 400 - 200 = 200$  MHz. All frequencies are normalized in the calculation. The signal with noise can be represented as:

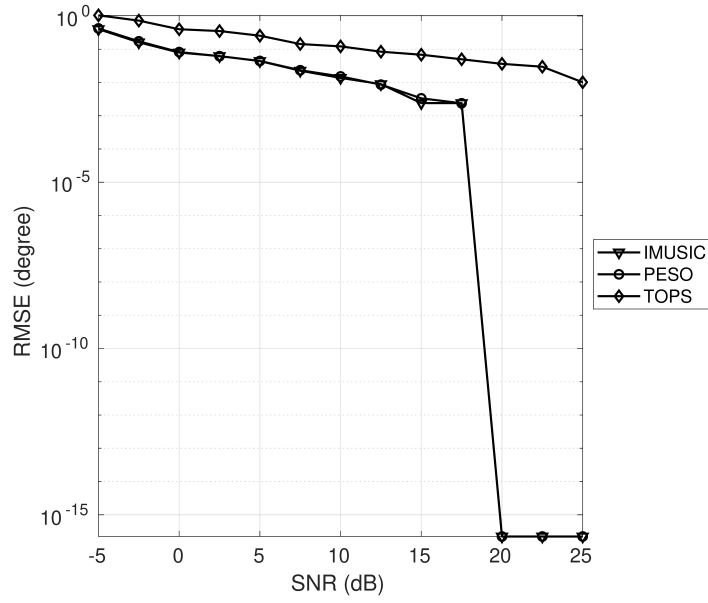


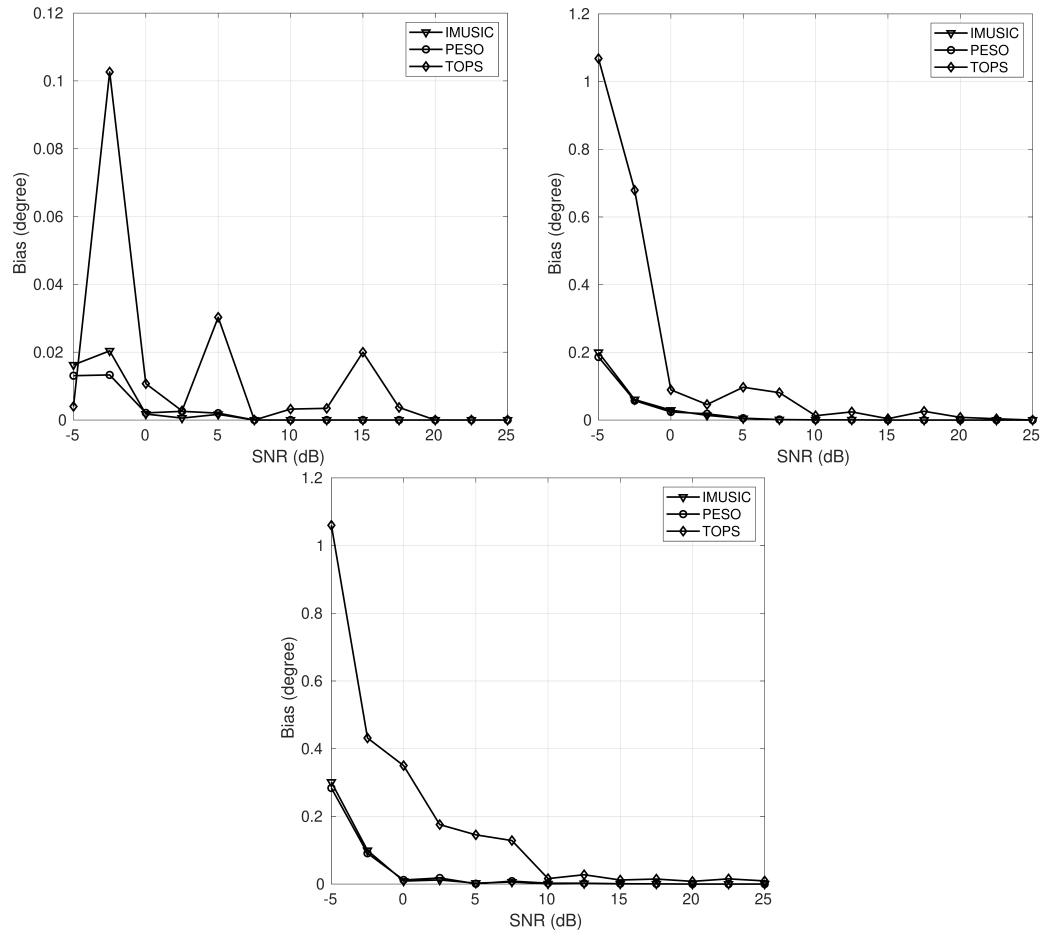
**Figure 2.13:** Total RMS Error for all three detected wideband sources at  $30^\circ$ ,  $50^\circ$  and  $65^\circ$ .

$$s_i(t) = \sum_{j=1}^L g_i(t) \exp(j2\pi f_j t) + n_i(t). \quad (2.50)$$

The variable  $g_i(t)$  represents the Gaussian random variable and  $n_i(t)$  represents the AWGN. The aim is to subdivide the frequency band. Therefore, FFT applied to the wideband signal. The subdivided a number of frequency bins  $L = 22$  for all DOA methods. The performance of the newly introduced method was tested with a low number (30) snapshots corresponding to the 128 FFT points.

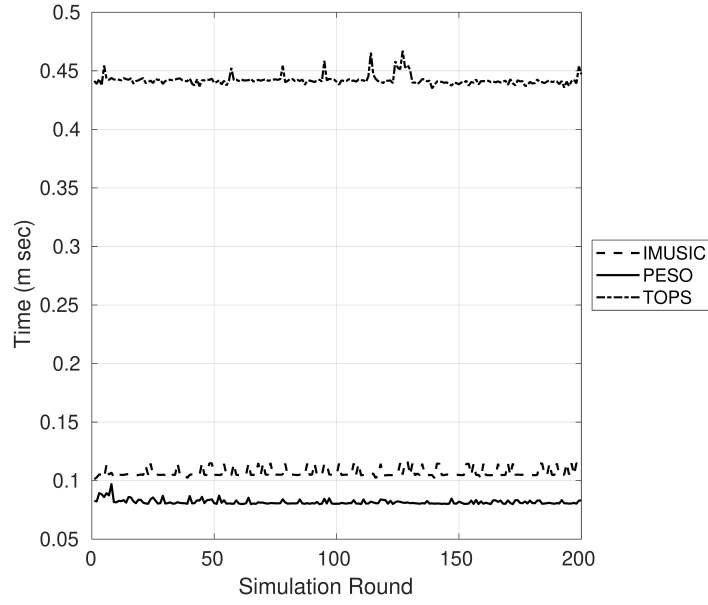
Fig. 2.11 shows the comparison results of PESO, IMUSIC, TOPS methods. The simulation was tested with very low SNR values of -5 dB and -2.5 dB. The PESO method produces very accurate results whereas IMUSIC and TOPS methods produce errors due to fluctuations at wrong angles. The advantage of the PESO method is due to the assignment of the probability of resolution such that any detection with a small range of error sets the probability to 1. This ensures to capture all related signals even with the smallest amplitude.

Fig. 2.12 demonstrates the probability of resolution measured at each SNR value for all simulation runs. Locations are accurately resolved with the PESO method. It is important to note the accuracy of the PESO method especially at low SNR values while other methods



**Figure 2.14:** Bias of the sources at (a)  $30^\circ$ , (b)  $50^\circ$ , and (c)  $65^\circ$  for the proposed method PESO, IMUSIC and TOPS methods.





**Figure 2.15:** Mean consumed time for 200 simulation rounds by the calculations of the proposed method PESO, IMUSIC and TOPS methods.

suffer under such conditions. This is due to frequency selection at the initial stage.

Fig. 3.3 indicates the total RMSE for all sources under test. The total RMSE can be calculated as:

$$RMSE = \frac{1}{D} \sum_{i=1}^D \sqrt{\frac{1}{200} \sum_{r=1}^{200} |\theta_i - \hat{\theta}_{i,r}|^2}. \quad (2.51)$$

$\theta_i$  represents the  $i$ th true DOA and  $\hat{\theta}_{i,r}$  represents the  $i$ th estimated DOA angle at the  $r$ th simulation round. The PESO method can accurately detect the DOA but TOPS method performs badly. This is because the minimum number of snapshots was used in processing.

Fig. 3.4 indicate the bias of the three sources at  $30^\circ$ ,  $50^\circ$  and  $65^\circ$ . The PESO method is compared with IMUSIC and TOPS methods. The PESO method has the lowest bias. The TOPS method achieves low bias at -5 dB. The accuracy of the PESO method is much better even at very low SNR ( $\leq 0$  dB). The PESO and IMUSIC produce accurate DOA values at high SNR values ( $\geq 10$  dB) with 0 bias. The PESO method produces higher resolution and accuracy to detect all emitting sources from the first execution. This makes the PESO method more reliable and practical.

Fig. 2.15 indicates the execution time for the compared methods. The PESO method takes the least execution time for all simulations. The mean execution time for the IMUSIC method is 0.107 msec and the mean execution time for the TOPS method is 0.442 msec. The mean execution time for PESO is 0.081 msec. The minimum execution time for the PESO algorithm is because it determines the correct DOAs first before it evaluates the average of the spatial spectrum for all frequency bins. This process results in minimum execution time as indicated in Fig. 2.15.

#### **2.5.4 Conclusion**

This research introduces a new DOA estimation method for wideband signals. The newly introduced method adopts the statistical probability method to improve DOA estimation performance under extreme conditions such as low SNR values. The simulation results verify that the introduced method does not include false peaks in the spatial spectrum. The TOPS and Squared TOPS methods produce many false peaks. The accuracy and resolution performance superiority of the newly described method over the compared methods has been proven. The newly introduced method does not require any initial estimates that lead to high computational cost and inaccurate estimation of the DOA. The classical methods deteriorate to estimate the DOA at close emitting sources. This is because all received signals are classified as noise and rejected in the calculation. The newly introduced method overcomes all such problems and uses a very low number of snapshots in the calculation.

## CHAPTER 3

### NEW NARROWBAND DOA ESTIMATION TECHNIQUES

#### 3.1 Introduction

Localization in a security system is a great concern, especially in 5G wireless networks and beyond. Accurate localization has the advantage to eliminate deliberate attacks arriving from different sources. The aim is to determine the location of multiple RF intruders and jammers with minimum effort of computation. In this research, we present a precise DOA estimation method for narrowband signal and a novel approach for geographical localization of multiple unauthorized sources based on the probabilistic approach. The probabilistic based localization behaves like the process of identifying incoming signals' DOA with the maximum likelihood values. This process requires less computational effort and produce exact DOA value. The precision of transmitter localization can be increased by using multiple test points. We used three test points in this experiment. Each data was recorded with prior knowledge of the test points. Once the accurate angle of arrival determined, a linear line was drawn manually. The intersection of the lines identified the location of the transmitter. The localization process is simple to apply and does not require prior knowledge of the signal.

Mainly, this research has two contributions that can be summarized as;

- A novel DOA estimation method based on sub-spaces methods called Probabilistic Estimation of Several Signals (PRESS). The introduced method achieves higher accuracy in the lowest bias of the estimated DOA and the Lowest RMSE value among narrowband DOA estimation methods such as Multiple Signal Parameter Estimation (MUSIC), Total Least Square Estimation of Signal Parameters via Rotational Invariance Technique (TLS-ESPRIT), Propagator Method (PM) and Capon methods at very low SNR values.
- At a point of localizing the unknown signal source using 3 different DOA estimation from 3 different stationary arrays of antenna or fixed array on top of a moving vehicle

to estimate the geographical location of the source with high accuracy.

The newly introduced method produce almost exact results even at very low SNR values. The PRESS method provides higher resolution and DOA accuracy than current models. The simulation results show that the proposed method produces accurate localization concerning the most recent introduced algorithms. The simulation and numerical results show that the PRESS DOA estimation method can be applied directly to solve the localization issue with a significant improvement compared with traditional localization techniques.

### 3.2 Signal Model

Let's assume a ULA of  $M$  elements where the separation distance  $d$  between every two elements is half the wavelength  $\lambda$  of the highest frequency. Consider a  $D$  ergodic and stationary zero-mean Gaussian random processes signals impinging on the array and emitted from far-field sources. These signals assumed to be linearly independent and there is no correlation between them. The received signal is expressed by:

$$x_m(t) = s_k(t) \cdot e^{-j2\pi(m-1)d\sin(\theta_k)}, \quad (3.1)$$

$$x_m(t) = a_m(\theta_k) \cdot s_k(t), \quad (3.2)$$

where  $s_k(t)$  is the  $k$ th received signal power and  $a(\theta_k)$  is the exponential term multiplied by the signal power called the steering vector that includes the DOA of the  $k$ th signal (Chen et al., 2010). An AWGN is added at each array element. Thus, the signal model can be expressed in matrices form by:

$$\mathbf{X} = \mathbf{A}\mathbf{S} + \mathbf{N}, \quad (3.3)$$

where  $\mathbf{N}$  is a matrix of all noise vectors adds to the  $m$ th sensor.  $\mathbf{A}$  is the steering matrix given by:

$$\mathbf{A} = \begin{bmatrix} a(\theta_1) & a(\theta_2) & \dots & a(\theta_D) \end{bmatrix}^T. \quad (3.4)$$

To extract the DOA information, we calculate the covariance matrix  $[M \times M]$  of the data. However, due to difficulty in obtaining the real correlation matrix, the statistical expectation is estimated as following:

$$\hat{\mathbf{V}}_{xx} = \frac{1}{N} \sum_{i=1}^N \mathbf{X}(t_i) \mathbf{X}^H(t_i), \quad (3.5)$$

where  $N$  is the number of snapshots taken from sensors. This equation of the covariance matrix is the fundamental for all DOA estimation methods where all of them try to apply different techniques in order to estimate the DOA with high accuracy (Schmidt, 1986).

### 3.3 Conventional DOA Estimation Methods

Let's now apply the EVD to the covariance matrix and calculate (3.5) as:

$$\mathbf{V}_{xx} \mathbf{w}_r = e_r \mathbf{w}_r = \sigma^2 \mathbf{w}_r. \quad (3.6)$$

Its eigenvalues can be obtained and sorted descendingly. The first  $[M - D]$  eigenvalues stand for the incident signals while the rest smallest eigenvalues are considered as noises. The corresponding eigenvectors of the two eigenvalues sets are called signal subspace  $\mathbf{E}_s$  and noise subspace  $\mathbf{E}_n$  respectively and expressed by:

$$\mathbf{E}_s = \begin{bmatrix} W_1 & W_2 & \dots & W_D \end{bmatrix}, \quad (3.7)$$

$$\mathbf{E}_n = \begin{bmatrix} W_{D+1} & W_{D+2} & \dots & W_M \end{bmatrix}, \quad (3.8)$$

where  $W$  is the  $m$ th eigenvector of the covariance matrix (Paulraj et al., 1993).

#### 3.3.1 MUSIC

The MUSIC is a well-known DOA estimation method firstly introduced in (Schmidt, 1986). MUSIC method elementary idea is that the eigenvectors of noise subspace are orthogonal to the columns of steering matrix that are in the signal subspace. This means that nulling the corresponding noise subspace in the steering matrix will declare the DOA of incident signals

but due to the lack in snapshots, some noise will appear (ke Nie et al., 2016). The power spectrum for the MUSIC algorithm is:

$$\mathbf{F}(\theta) = \frac{1}{\mathbf{a}^H(\theta)\mathbf{E}_n\mathbf{E}_n^H\mathbf{a}(\theta)}. \quad (3.9)$$

When the denominator in (3.9) goes to zero for the true angles of the signals, the power spectrum will have peaks indicating this angles (Becker, Chevalier, & Haardt, 2017).

### 3.3.2 ESPRIT

Another well established DOA estimation method is ESPRIT and its improvements; Least square (LS-ESPRIT) and TLS-ESPRIT (Tayem, Omer, Gami, & Nayfeh, 2013) which basically subdivide the steering array to two well-displaced arrays that exploit the DOA information by taking the eigen decomposition of the estimated data covariance matrix mentioned in (3.5) and these two sub-arrays (Paulraj, Roy, & Kailath, 1986). The two sub-arrays will have a signal model is given by:

$$\mathbf{X}_1 = \mathbf{A}\mathbf{S} + \mathbf{N}_1, \quad (3.10)$$

$$\mathbf{X}_2 = \mathbf{A}\gamma\mathbf{S} + \mathbf{N}_2, \quad (3.11)$$

where  $\mathbf{N}_1$  and  $\mathbf{N}_2$  are the additive noise vectors added to the two arrays respectively, and  $\gamma$  is the rotation  $[M \times M]$  matrix expresses the displacement between the two arrays and defined by:

$$\gamma = \begin{bmatrix} z_1 & 0 & \dots & 0 \\ 0 & z_2 & \dots & 0 \\ \vdots & \vdots & \ddots & \vdots \\ 0 & 0 & \dots & z_M \end{bmatrix}, \quad (3.12)$$

where  $z_m = e^{j\lambda d \cos \theta_m}$  and  $d$  is the distance between the two arrays (Roy, Paulraj, & Kailath, 1986).

### 3.3.3 Capon

Capon method is one of the earliest introduced methods to solve the problem of DOA estimation and source localization (Capon, 1969; Stoica, Händel, & Söderström, 1995). It is similar to Maximum Likelihood. Capon method directly applied the minimum variance approach to the invert of the covariance matrix in order to achieve higher resolution than previous methods. The spatial spectrum of Capon calculated by:

$$\mathbf{F}(\theta) = \frac{1}{\mathbf{a}^H(\theta) \hat{\mathbf{V}}_{xx}^H \mathbf{a}(\theta)}, \quad (3.13)$$

where  $\hat{\mathbf{V}}_{xx}'$  is the invert of the covariance matrix (Tzafri & Weiss, 2016). Capon method performance suffers from high bias compared with other methods. Therefore, EVD methods still much better in terms of resolution and accuracy (Handel, Stoica, & Soderstrom, 1993).

### 3.3.4 PM

PM method firstly introduced in (Marcos, Marsal, & Benidir, 1995), which follows a approach analogical to ESPRIT method. PM method split the covariance matrix into two matrices. The first matrix  $U$  with dimension  $[M, 1 : D]$  and the second matrix  $V$  dimension will be  $[M, M - D : M]$  (Sun, Wang, & Pan, 2019).

$$\mathbf{G} = \frac{\mathbf{U}' \mathbf{V}}{\mathbf{U}' * \mathbf{U}}, \quad (3.14)$$

$$\mathbf{P} = [\mathbf{G}' - \mathbf{I}], \quad (3.15)$$

where  $\mathbf{I}$  is the identity matrix of dimension  $[M - D]$  (Shiying & Hongqiang, 2018). Finally, The spatial spectrum of PM is calculated by

$$\mathbf{F}(\theta) = \frac{1}{\mathbf{a}^H(\theta) \mathbf{P}^H \mathbf{P} \mathbf{a}(\theta)}. \quad (3.16)$$

### 3.4 The Proposed Method

The introduced methodology consists of two stages. Firstly, it estimates the DOA using a new method. Secondly, using a DOA estimation from different locations, the geographical location of the sources can be revealed with high accuracy. In general, DOA methods give the direction from where the signal impinging on the array of sensors. However, it is possible using three different sets of arrays as it is the minimum number to estimate the location of the signals within a considerable range, especially for very close sources. In this section, firstly, the novel DOA method called PRESS is introduced. Secondly, the localization algorithm is presented.

#### 3.4.1 PRESS DOA Estimation Method

The proposed DOA method exploits the spatio-temporal information within the sensor data before drawing the final spatial spectrum. First, the conventional subspace estimation for narrowband signal is calculated by

$$\mathbf{Q} = \mathbf{a}^H(\theta) \mathbf{E}_n \mathbf{E}_n^H \mathbf{a}(\theta), \quad (3.17)$$

where  $\mathbf{E}_n$  is the noise subspace expressed by (3.8) and  $\mathbf{a}(\theta)$  is the steering vector. Inspired by the accuracy enhancement done in TOPS method and its latest developments for wideband signal (Bilgehan & Abdelbari, n.d.), the accuracy of (3.17) is enhanced by the projection of steering vectors as follows:

$$\mathbf{R} = \mathbf{H} * \mathbf{Q}, \quad (3.18)$$

where

$$\mathbf{H} = \mathbf{I} - \frac{\mathbf{a} * \mathbf{a}^H}{\mathbf{a}^H * \mathbf{a}}, \quad (3.19)$$

where  $\mathbf{I}$  is the identity matrix of dimension  $[M - M]$ . Although the estimation in (3.18) is much better than usual DOA methods, the side false peaks are very high and affecting the estimation dramatically. Thus, another calculation is applied by multiplying the signal subspace  $\mathbf{E}_s$  expressed by (3.7) to reduce these peaks as follows:



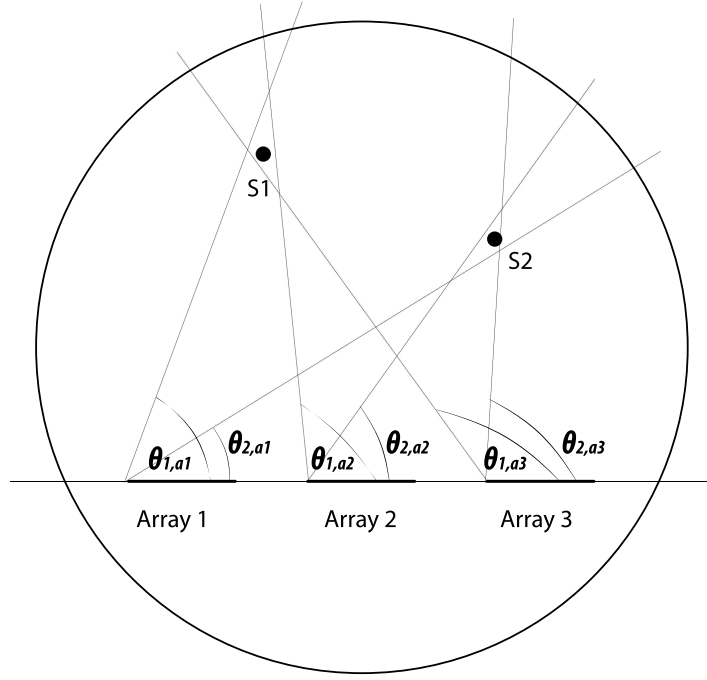


**Figure 3.1:** Visual illustration of localization algorithm using 3 arrays to locate two sources. S1 and S2 are the locations of the sources 1 and 2 respectively.  $\theta_{1,a1}$  and  $\theta_{2,a1}$  are the estimated DOA at the first array from the S1 and S2, respectively.  $\theta_{1,a2}$  and  $\theta_{2,a2}$  are the estimated DOA at the second array from the S1 and S2, respectively.  $\theta_{1,a3}$  and  $\theta_{2,a3}$  are the estimated DOA at the third array from the S1 and S2, respectively.

$$\mathbf{Z} = \mathbf{H}^H * (\mathbf{E}_s * \mathbf{E}_s^H) * \mathbf{H}. \quad (3.20)$$

Finally, the SVD is applied to (3.20) for each hypothesis search angle  $\theta$  and taking the least singular value  $\mu(\theta)$ . The PRESS Spatial Spectrum can be calculated by:

$$\mathbf{F}(\theta) = \arg \max \left\{ \frac{1}{\min\{\mu(\theta)\}} \right\}. \quad (3.21)$$

### 3.4.2 Localization Algorithm

For the source geographical locating approach, at least three observations have to be taken from three different known locations of either three fixed array of sensors or a moving vehicle with fixed array on top of it.

Let's assume the general case where a three array located at the same baseline where their geographical location is known. Each array has a ULA geometry. The displacement between

each array is also known to the observer. In Fig. 3.1, an example of locating two sources where each array estimates the DOA from its observation point. In an ideal case, the lines of DOAs for single source assumed to intersect at the same point. However, in practice, there is a bias from the exact DOA measured by each array. This is illustrated in Fig. 3.1, where the DOAs form a small triangle around the location of each source. Further, by putting this measurement into a map of the covered area, the estimated geographical location ( longitude and latitude ) of the source can be revealed.

Assume a set of estimated DOAs for the  $i$ th source of the  $v$ th array given by:

$$\Theta_{i,v} = \begin{bmatrix} \theta_{1,1} & \theta_{1,2} & \cdots & \theta_{1,v} & \cdots & \theta_{1,V} \\ \theta_{2,1} & \theta_{2,2} & \cdots & \theta_{2,v} & \cdots & \theta_{2,V} \\ \vdots & \vdots & \vdots & \vdots & \vdots & \vdots \\ \theta_{D,1} & \theta_{D,2} & \cdots & \theta_{i,v} & \cdots & \theta_{D,V} \end{bmatrix}, \quad (3.22)$$

where  $V$  is the number of arrays and  $D$  is the number of sources. From the assumption that the first element of the array is the reference, a line can be drawn for the  $i$ th source of the  $v$ th array by calculating the full angles of each triangle using the DOA information and getting the distance from each array using the basics of trigonometry. The calculation for the first source is as follow

$$\frac{\sin(\theta_{1,1})}{R_{1,2}} = \frac{\sin(\pi - \theta_{1,2})}{R_{1,1}} = \frac{\sin(\gamma_{1,1})}{d_1}, \quad (3.23)$$

$$\frac{\sin(\theta_{1,2})}{R_{1,3}} = \frac{\sin(\pi - \theta_{1,3})}{R_{1,2}} = \frac{\sin(\gamma_{1,2})}{d_2}, \quad (3.24)$$

where  $R_{1,1}$  is the distance from the 1st array to the 1st source,  $R_{1,2}$  is the distance from the 2nd array to the 1st source,  $R_{1,3}$  is the distance from the 3rd array to the 1st source,  $d_1$  is the distance between 1st and 2nd arrays, and  $d_2$  is the distance between 2nd and 3rd arrays.  $\gamma_{1,1}$  denotes the angle in front of  $d_1$  in the triangle [array 1, S1, array 2] and  $\gamma_{1,2}$  denotes the angle in front of  $d_2$  in the triangle [array 2, S1, array 3]. Then, the distances  $R_{1,1}$ ,  $R_{1,2}$ , and  $R_{1,3}$  can be calculated as follow

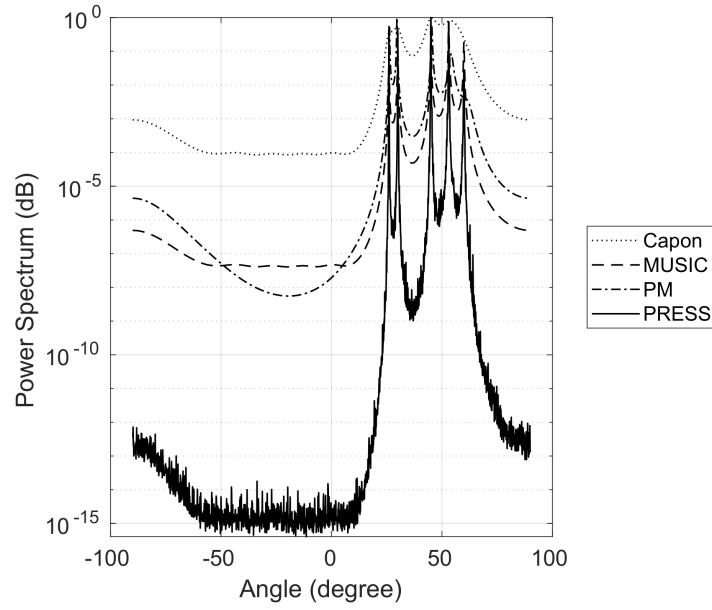


**Figure 3.2:** Normalized spatial spectrum at -5dB for PRESS, MUSIC, PM, and Capon methods for sources at  $26^\circ$ ,  $30^\circ$ ,  $45^\circ$ ,  $53^\circ$ , and  $60^\circ$ .

$$R_{1,1} = \frac{d_1 \cdot \sin(\pi - \theta_{1,2})}{\sin(\gamma_{1,1})}, \quad (3.25)$$

$$R_{1,2} = \frac{d_1 \cdot \sin(\theta_{1,1})}{\sin(\gamma_{1,1})} = \frac{d_2 \cdot \sin(\pi - \theta_{1,3})}{\sin(\gamma_{1,2})}, \quad (3.26)$$

$$R_{1,3} = \frac{d_2 \cdot \sin(\theta_{1,2})}{\sin(\gamma_{1,2})}. \quad (3.27)$$

Furthermore, by inserting this information into a map or estimation the triangle around the source location. The aforementioned calculations can be easily done for other sources. Also, it's easy to implement in real localization devices for different application.

### 3.4.3 The PRESS algorithm

For DOA estimation, the PRESS algorithm defined as:

- **Step 1:** Calculate the covariance matrix using (3.5) for the  $l$ th set of snapshots and apply the eigenvalue decomposition to get the signal subspace and noise subspace in (3.7) and (3.8).

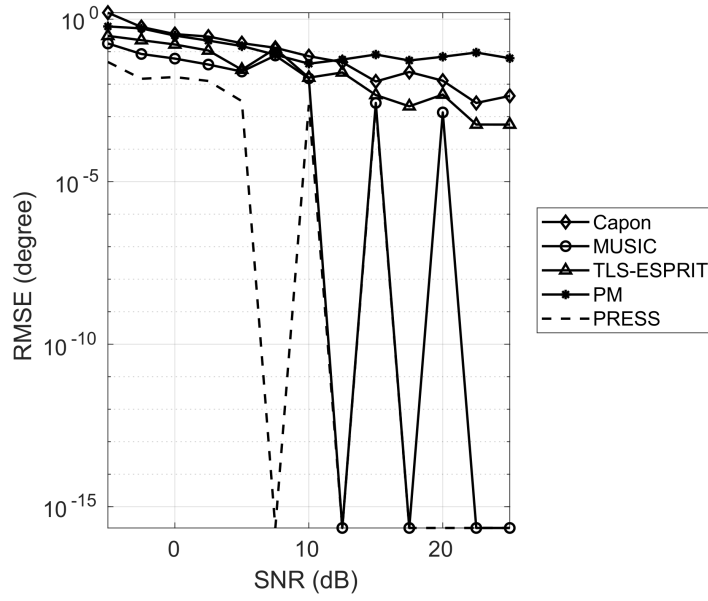


**Figure 3.3:** Total RMSE measured from -5dB to 25dB values of SNR for PRESS, MUSIC, TLS-ESPRIT, PM, and Capon methods for five sources located at  $26^\circ$ ,  $30^\circ$ ,  $45^\circ$ ,  $53^\circ$ , and  $60^\circ$ .

- **Step 2:** Calculate (3.17), (3.18) and (3.20).
- **Step 3:** Find the minimum singular value for each hypothesis angle and plot the spatial spectrum using (3.21).

For source localization, the algorithm will be:

- **Step 1:** Estimate the DOA of the  $i$ th source using a minimum of three arrays.
- **Step 2:** Place the location of the  $v$ th array on the map and draw a linear line corresponding to the  $\theta_{i,v}$ .
- **Step 3:** The location of the  $i$ th source can be determined as the intersection of the  $V$  lines.

### 3.5 Simulation Results

To evaluate the performance of the PRESS DOA estimation and localization algorithm, a Monte-Carlo simulation has been run for 250 trials on MATLAB (version 2018a) and one study case emulated for the localization algorithm. Let's assume a ULA of  $M = 10$  elements displaced by a normalized distance  $d = 0.5$ . The  $D = 5$  sources for the simulation are located under the far-field assumption at  $[26^\circ, 30^\circ, 45^\circ, 53^\circ, \text{ and } 60^\circ]$ . The normalized

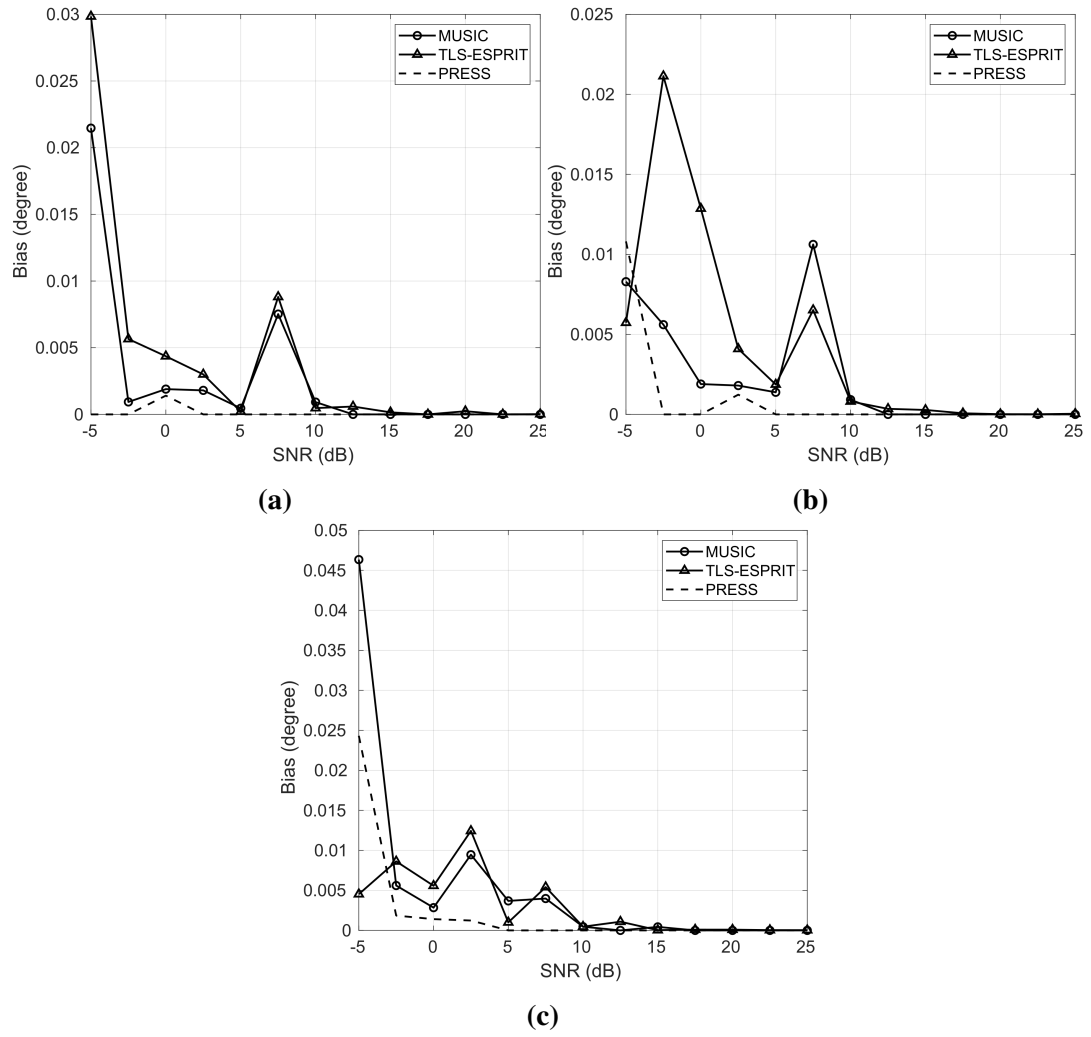


**Figure 3.4:** Bias of the source at: (a)  $26^\circ$ , (b)  $30^\circ$ , and (c)  $60^\circ$ , for PRESS, MUSIC, and TLS-ESPRIT methods.

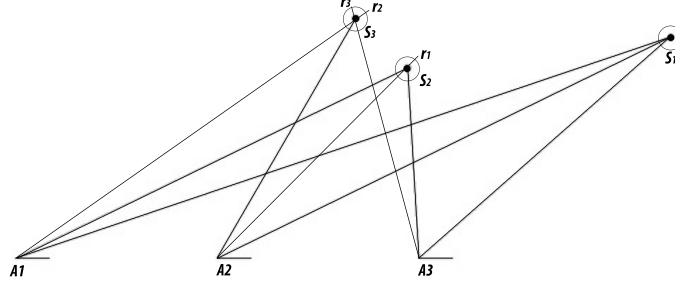


**Figure 3.5:** The case study of localization algorithm in which it locates three sources at three different locations using three arrays.

frequencies of the 5 sources are  $[\pi/4, \pi/3, 2/3\pi, \pi, \text{ and } 5/4\pi]$ . The received signal can be expressed by

$$s_i(t) = g_i(t)e^{j2\pi f_c t} + n_i(t), \quad (3.28)$$

where  $g_i(t)$  is a Gaussian random variable that represents the magnitude of the signal and  $n_i(t)$  is a random variable representing the AWGN. The number of snapshots is taken for both the simulation trials and the case study is  $N = 10,000$  for all DOA methods to demonstrate the effectiveness and novelty of the PRESS method.

Fig. 3.2 shows a significant enhancement in the resolution of the spatial spectrum of the PRESS method compared with the traditional DOA methods even at very low SNR value (-5 dB) for all sources and especially for very close sources at  $26^\circ$  and  $30^\circ$ . Capon and PM method performance degrades as the SNR decreases dramatically and can not estimate all the DOAs while MUSIC method performance still robust and acts well at low SNR. Despite that, Fig. 3.2 clearly shows the superior of the PRESS method resolution even with the observed low level of noise that appears in the spectrum. This noise actually appears at very low dB ( $< 10^{-11}$ dB) and does not affect the accuracy of the estimation as other analysis metrics prove.

Fig. 3.3 shows the total RMSE for all sources. Obviously, the performance of subspace methods; MUSIC and TLS-ESPRIT are much better than the performance of Capon and PM methods. However, due to the deep exploit of the probabilistic in PRESS method, it achieves the lowest estimation error ever in low SNR values ( $< 10$ dB). In high SNR values,

the performance of PRESS method is similar to the MUSIC method which still better than other existing methods.

Fig. 3.4 illustrates the absolute bias from the correct DOA of  $26^\circ$ ,  $30^\circ$ , and  $60^\circ$  angles separately which has been averaged over the number of simulation trials. Here, the performance of PRESS method is compared with only the two high-resolution methods; MUSIC and TLS-ESPRIT to make the presentation of the results clear and intensive. Firstly, the bias for all DOAs of all methods is very low ( $< 0.05$ ) due to the high number of snapshots. Secondly, the effectiveness of TLS-ESPRIT is still less than MUSIC which is comprehensible from Fig. 3.4a, and 3.4b. However, the performance can be very close or even better in some cases which can be seen from some overcome of TLS-ESPRIT performance in low SNR values. This is because the resolution degrades dramatically and in some cases, the DOA method can't estimate all sources with the same accuracy. For PRESS method, Fig. 3.4 shows the supreme and noteworthy performance for all sources which does not exceed 0.025 at the most in the extreme SNR value -5 dB. Moreover, the outstanding performance of PRESS method observed in the estimation precise for all DOAs that makes PRESS method robust against noise and not affect by the low SNR.

The complexity of the PRESS method compared to other stimulated methods is measured by calculating the averaged elapsed time taken by each algorithm. The averaged elapsed time for Capon is  $3.08 * 10^{-03}$  msec, for MUSIC is  $2.20 * 10^{-03}$  msec, for TLS-ESPRIT is  $4.41 * 10^{-05}$  msec, for PM is  $1.78 * 10^{-03}$  msec, and for PRESS is  $1.26 * 10^{-02}$  msec. Due to the calculation of SVD at every hypothesis angle, PRESS method suffers from slightly high computational costs in comparison with other methods.

**Table 3.1:** Bias of PRESS method at -5dB for the three sources measured from three separated locations.

Location No.	$\theta_1$	Bias	$\theta_2$	Bias	$\theta_3$	Bias
1st location	$19^\circ$	$0^\circ$	$26^\circ$	$0^\circ$	$35^\circ$	$0.0008^\circ$
2nd location	$26^\circ$	$0^\circ$	$45^\circ$	$0.006^\circ$	$60^\circ$	$0^\circ$
3rd location	$41^\circ$	$0^\circ$	$-3^\circ$	$0^\circ$	$-15^\circ$	$0.0002^\circ$

The localization algorithm tested with a case study. Firstly, three different locations were selected to record the data received from 3 sources at -5 dB. To be practical, the sensors data

is recorded for 3000 snapshots. Secondly, the PRESS DOA estimation has been applied and the bias is shown in Tab. 3.1. The newly introduced method illustrates very low bias (as low as zero) in some observations. The low bias leads to a precise estimation of the source location. In Fig. 3.5, the localization of three sources at three different locations can be accurately determined. It is shown that source  $S_1$  has been locked on its location with zero bias. For the second  $S_2$  and third  $S_3$  sources, the bias is infinitesimal according to Tab. 3.1 and shown in Fig. 3.4 as  $r_1, r_2$  and  $r_3$  that can be assumed as zero and their locations are declared without any errors. The newly introduced algorithm performs best among the existing localization algorithms. The new algorithm produces the least average error compared with source locating (1.83 m) algorithm in (Bulusu, Heidemann, & Estrin, 2000) and has smaller bias circle than ( $> 0.2^\circ$ ) in (Han, Xu, Duong, Jiang, & Hara, 2013) around each source (Nazir, Shahid, Arshad, & Raza, 2012) (Jiang, Wang, & Zhang, 2018).

### 3.6 Conclusion

Localization has always been an important part of the security systems in wireless networks like cellular networks and WSN. There are many algorithms introduced to overcome such a problem, but they are both complex to handle based on resource constraints and involving a large estimation error. The proposed DOA estimation method assigns probabilistic values to related peaks. Therefore, the uncorrelated peaks have small probabilistic values that can easily be identified. The second important contribution is the biasing in spatial analysis kept very narrow so most of the uncorrelated signal components are not involved in the calculation process. This reduces the computational cost to low limits. The simulation results show that the newly introduced PRESS method produces an accurate localization for multiple sources. The PRESS method can be successfully used to overcome the problem of attacks arriving at the emitter and it is suitable for dynamic environments. More experimental studies are needed to demonstrate and implement the localization of RF sources using DOA information in practice which will have a great impact in many applications.



## CHAPTER 4

### CONCLUSIONS AND FUTURE WORK

#### 4.1 Conclusions

The aims of any localization method is to localize multiple targets accurately to a certain level with the minimum complexity. This is to overcome the issue of tracking each target separately which consume resources dramatically as the number of targets increase. Another issue is the time consumed to locate the targets can be repeated continuously in case of moving targets to track their movements. The localization algorithm should be at low latency to be effective and practical.

The DOA estimation is very effective in the localizing the origin or source of any signal from any type. This is useful in understanding both the source and the signal better. Also, it has many applications in several fields such as wireless networks, astronomy, radars, sonars, seismology, and military surveillance. DOA is an estimation problem which tries to reveal the underlying parameters in the sensors data using different mathematical techniques, the geometry of the array of antenna, and the characteristics of the received signals. Matrix multiplication and manipulation are almost the core of the exploitation of the DOA information e.g. matrix sub-spaces orthogonality, eigen compensation, and singular value decomposition. Due to the natural differences between narrowband and wideband signals, the DOA estimation of both signals is different and so the methods estimating the DOA in a narrowband are not sufficient for wideband DOA estimation. Wideband DOA methods are classified into two main categories; incoherent e.g. IMUSIC and coherent methods e.g. CSS, WAVES and TOPS. However, the existing method did not address the issues of wrong estimation, high bias, high complexity, unknown characteristics of the sources, revealing the location based on the estimated DOA.

In this thesis, such issues have been addressed. Several contributions including narrowband and wideband DOA estimation methods proposed in the research that use different techniques to achieve a high-resolution estimation while maintaining low computational costs.

The finding in this thesis shows that there are some dominant factors controlling the complexity of each algorithm. Exploring this factors within the well known DOA methods while maintaining a high resolution is investigated through the results and discussion.

## **4.2 Future Work**

A hardware implementation of an application-based localization system that uses one of the recent DOA estimation algorithms with array of sensor suitable for those specific applications. For instance, a localization device for the next generation mobile network which help on locating and hence, optimizing the power, bandwidth for each mobile user.

Another future work is the studying of moving objects and the effect of its characteristics on the localization process. For instance, in medical field, the localization of humans based on heart beats or in astronomy, the localization of stars based on the emitted electromagnetic signals. Such objects encounter very different movement characteristics which may affect the localization significantly.

## REFERENCES

- Abdelbari, A. (2018). *Direction of arrival estimation of wideband RF sources* (Unpublished master's thesis). Near East University.
- Abdelbari, A., & Bilgehan, B. (2020a). A novel doa estimation method of several sources for 5g networks. In *2020 international conference on electrical, communication, and computer engineering (icecce)* (p. 1-6). doi: 10.1109/ICECCE49384.2020.9179306
- Abdelbari, A., & Bilgehan, B. (2020b). A probabilistic-based approach for direction-of-arrival estimation and localization of multiple sources. *International Journal of Communication Systems*, 33(11), e4425. (e4425 dac.4425) doi: 10.1002/dac.4425
- Abdelbari, A., & Bilgehan, B. (2021). PESO: probabilistic evaluation of subspaces orthogonality for wideband DOA estimation. *Multidimens. Syst. Signal Process.*, 32(2), 715–746. doi: 10.1007/s11045-020-00757-6
- Abdelbari, A., & Haci, H. (2019a). Fuzzy logic-based user scheduling scheme for 5g wireless networks and beyond. In *International conference on theory and application of soft computing, computing with words and perceptions* (pp. 429–435).
- Abdelbari, A., & Haci, H. (2019b). An opportunistic user scheduling scheme for ultra-dense wireless networks. In *2019 11th international conference on electrical and electronics engineering (eleco)* (p. 1080-1084). doi: 10.23919/ELECO47770.2019.8990469
- Aboutanios, E., Hassanien, A., El-Keyi, A., Nasser, Y., & Vorobyov, S. (2017, 08). Advances in doa estimation and source localization. *International Journal of Antennas and Propagation*, 2017, 1-3. doi: 10.1155/2017/1352598
- Akyildiz, I., Su, W., Sankarasubramaniam, Y., & Cayirci, E. (2002). Wireless sensor networks: a survey. *Computer Networks*, 38(4), 393 - 422. doi: 10.1016/S1389-1286(01)00302-4
- Balanis, C. (2007). *Introduction to smart antennas* (1st ed.). Morgan and Claypool Publishers.
- Becker, H., Chevalier, P., & Haardt, M. (2017). Higher order direction finding from rectangular cumulant matrices: The rectangular 2q-music algorithms. *Signal Processing*, 133, 240 - 249. doi: 10.1016/j.sigpro.2016.10.020
- Bilgehan, B., & Abdelbari, A. (n.d.). Fast detection and doa estimation of the unknown wideband signal sources. *International Journal of Communication Systems*, 0(0), e3968. (e3968 dac.3968) doi: 10.1002/dac.3968

- Bilgehan, B., & Abdelbari, A. (2019a). Fast detection and doa estimation of the unknown wideband signal sources. *International Journal of Communication Systems*, 32(11), e3968. (e3968 dac.3968) doi: 10.1002/dac.3968
- Bilgehan, B., & Abdelbari, A. (2019b). A novel doa estimation method for wideband sources based on fuzzy systems. In *International conference on theory and application of soft computing, computing with words and perceptions* (pp. 405–412).
- Bulusu, N., Heidemann, J., & Estrin, D. (2000, Oct). Gps-less low-cost outdoor localization for very small devices. *IEEE Personal Communications*, 7(5), 28-34. doi: 10.1109/98.878533
- Candes, E. J., Romberg, J., & Tao, T. (2006, Feb). Robust uncertainty principles: exact signal reconstruction from highly incomplete frequency information. *IEEE Transactions on Information Theory*, 52(2), 489-509. doi: 10.1109/TIT.2005.862083
- Capon, J. (1969, Aug). High-resolution frequency-wavenumber spectrum analysis. *Proceedings of the IEEE*, 57(8), 1408-1418. doi: 10.1109/PROC.1969.7278
- Carreira-Perpiñán, M. Á. (2015). A review of mean-shift algorithms for clustering. *CoRR*, abs/1503.00687. Retrieved from <http://arxiv.org/abs/1503.00687>
- Chen, Z., Gokeda, G., & Yu, Y. (2010). *Introduction to direction-of-arrival estimation*. Artech House.
- Cheng, Y., Yu, R., Gu, H., & Su, W. (2013). Multi-svd based subspace estimation to improve angle estimation accuracy in bistatic mimo radar. *Signal Processing*, 93(7), 2003 - 2009. doi: 10.1016/j.sigpro.2012.12.021
- del Peral-Rosado, J. A., Raulefs, R., López-Salcedo, J. A., & Seco-Granados, G. (2018, Secondquarter). Survey of cellular mobile radio localization methods: From 1g to 5g. *IEEE Communications Surveys Tutorials*, 20(2), 1124-1148. doi: 10.1109/COMST.2017.2785181
- di Claudio, E. D., & Parisi, R. (2001, Oct). Waves: weighted average of signal subspaces for robust wideband direction finding. *IEEE Transactions on Signal Processing*, 49(10), 2179-2191. doi: 10.1109/78.950774
- Ebadi, Z., & Moghaddam, S. S. (2017). Modified rotational signal subspace algorithm. In *2017 international conference on wireless communications, signal processing and networking (wispnet)* (p. 2557-2560).
- el Ouargui, I., Frikel, M., & Said, S. (2018, 05). Comparative study between wideband doa estimation algorithms: Tct, tops, w-cmsr. In *International conference on signals, automation and telecommunications - icast'2018*. Beni-Mellal, Morocco.

- Haci, H., & Abdelbari, A. (2019). A novel scheduling scheme for ultra-dense networks. In *2019 international symposium on networks, computers and communications (isncc)* (p. 1-6). doi: 10.1109/ISNCC.2019.8909118
- Haci, H., & Abdelbari, A. (2020). Throughput enhanced scheduling (tes) scheme for ultra-dense networks. *International Journal of Communication Systems*, 33(4), e4229. (e4229 dac.4229) doi: 10.1002/dac.4229
- Han, G., Xu, H., Duong, T. Q., Jiang, J., & Hara, T. (2013, Apr 01). Localization algorithms of wireless sensor networks: a survey. *Telecommunication Systems*, 52(4), 2419–2436. doi: 10.1007/s11235-011-9564-7
- Handel, P., Stoica, P., & Soderstrom, T. (1993, Jan). Capon method for doa estimation: accuracy and robustness aspects. In *Ieee winter workshop on nonlinear digital signal processing* (p. 1-5). doi: 10.1109/NDSP.1993.767766
- Hayashi, H., & Ohtsuki, T. (2016, Oct 12). Doa estimation for wideband signals based on weighted squared tops. *EURASIP Journal on Wireless Communications and Networking*, 2016(1), 243. doi: 10.1186/s13638-016-0743-9
- Haykin, S., & Veen, B. V. (2002). *Signals and systems* (2nd ed.). USA: John Wiley & Sons, Inc.
- Hehdly, K., Laaraiedh, M., Abdelkefi, F., & Siala, M. (n.d.). Cooperative localization and tracking in wireless sensor networks. *International Journal of Communication Systems*, 32(1), e3842. (e3842 dac.3842) doi: 10.1002/dac.3842
- Jiang, R., Wang, X., & Zhang, L. (2018, 10). Localization algorithm based on iterative centroid estimation for wireless sensor networks. *Mathematical Problems in Engineering*, 2018, 1-11. doi: 10.1155/2018/5456191
- Karp, B., & Kung, H. T. (2000). Gpsr: Greedy perimeter stateless routing for wireless networks. In *Proceedings of the 6th annual international conference on mobile computing and networking* (p. 243–254). New York, NY, USA: Association for Computing Machinery. doi: 10.1145/345910.345953
- ke Nie, W., zheng Feng, D., Xie, H., Li, J., & fei Xu, P. (2016). Improved music algorithm for high resolution angle estimation. *Signal Processing*, 122, 87 - 92. doi: 10.1016/j.sigpro.2015.12.002
- Kulhandjian, H., Kulhandjian, M., Kim, Y., & D'Amours, C. (2018). 2-d doa estimation of coherent wideband signals with auxiliary-vector basis. In *2018 ieee international conference on communications workshops (icc workshops)* (p. 1-6).
- Lee, H. B., & Wengrovitz, M. S. (1991, June). Statistical characterization of the music null spectrum. *IEEE Transactions on Signal Processing*, 39(6), 1333-1347. doi: 10.1109/78.136540

- Liao, W., & Fannjiang, A. (2016). Music for single-snapshot spectral estimation: Stability and super-resolution. *Applied and Computational Harmonic Analysis*, 40(1), 33 - 67. doi: 10.1016/j.acha.2014.12.003
- Liu, D., & Ning, P. (2003). Location-based pairwise key establishments for static sensor networks. In *Proceedings of the 1st acm workshop on security of ad hoc and sensor networks* (p. 72–82). New York, NY, USA: Association for Computing Machinery. doi: 10.1145/986858.986869
- Liu, J., Mallick, M., Lian, F., Han, C., Sheng, M., & Yao, X. (2015). General similar sensing matrix pursuit: An efficient and rigorous reconstruction algorithm to cope with deterministic sensing matrix with high coherence. *Signal Processing*, 114, 150 - 163. doi: 10.1016/j.sigpro.2015.03.002
- Lv, S., & Liu, J. (2013). A novel signal separation algorithm based on compressed sensing for wideband spectrum sensing in cognitive radio networks. *International Journal of Communication Systems*, 27(11), 2628-2641. doi: 10.1002/dac.2495
- Marcos, S., Marsal, A., & Benidir, M. (1995). The propagator method for source bearing estimation. *Signal Processing*, 42(2), 121 - 138. doi: 10.1016/0165-1684(94)00122-G
- Marinho, M. A., Antreich, F., Caizzone, S., da Costa, J. P. C., Vinel, A., & de Freitas, E. P. (2018). Robust nonlinear array interpolation for direction of arrival estimation of highly correlated signals. *Signal Processing*, 144, 19 - 28. doi: 10.1016/j.sigpro.2017.09.025
- Monzingo, R., Haupt, R., & Miller, T. (2011). *Introduction to adaptive arrays*. Institution of Engineering and Technology.
- Munir, K., Zahoor, E., Rahim, R., Lagrange, X., & Lee, J. (2018). Secure and fault-tolerant distributed location management for intelligent 5g wireless networks. *IEEE Access*, 6, 18117-18127. doi: 10.1109/ACCESS.2018.2808333
- Naser, N., & Abdelbari, A. (2020). Estimation of global solar radiation using back propagation neural network: A case study tripoli, libya. In *2020 international conference on electrical, communication, and computer engineering (icecce)* (p. 1-5). doi: 10.1109/ICECCE49384.2020.9179201
- Nazir, U., Shahid, N., Arshad, M. A., & Raza, S. H. (2012, Dec). Classification of localization algorithms for wireless sensor network: A survey. In *2012 international conference on open source systems and technologies* (p. 1-5). doi: 10.1109/ICOSST.2012.6472830
- Nicoliche, C. Y. N., Oliveira, O. N., & Lima, R. S. (2020). Chapter 9 - multidimensional sensors: Classification, nanopores, and microfluidics. In C. M. Hussain (Ed.), *Handbook*

*on miniaturization in analytical chemistry* (p. 185-219). Elsevier. doi: 10.1016/B978-0-12-819763-9.00009-X

- Obeidat, H., Shuaieb, W., Obeidat, O., & Abd-Alhameed, R. (2021, 02). A review of indoor localization techniques and wireless technologies. *Wireless Personal Communications*. doi: 10.1007/s11277-021-08209-5
- Paulraj, A., Ottersten, B., Roy, R., Swindlehurst, A., Xu, G., & Kailath, T. (1993, jan). *16 Subspace methods for directions-of-arrival estimation* (Vol. 10). Elsevier. doi: 10.1016/S0169-7161(05)80082-3
- Paulraj, A., Roy, R., & Kailath, T. (1986, July). A subspace rotation approach to signal parameter estimation. *Proceedings of the IEEE*, 74(7), 1044-1046. doi: 10.1109/PROC.1986.13583
- Roy, R., Paulraj, A., & Kailath, T. (1986, October). Esprit—a subspace rotation approach to estimation of parameters of cisoids in noise. *IEEE Transactions on Acoustics, Speech, and Signal Processing*, 34(5), 1340-1342. doi: 10.1109/TASSP.1986.1164935
- Rudnitskaya, A. (2019). Sensors — biomimetic sensor arrays. In P. Worsfold, C. Poole, A. Townshend, & M. Miró (Eds.), *Encyclopedia of analytical science (third edition)* (Third Edition ed., p. 154-160). Oxford: Academic Press. doi: 10.1016/B978-0-12-409547-2.13935-6
- Salamah, M., & Doukhitch, E. (n.d.). An efficient algorithm for mobile objects localization. *International Journal of Communication Systems*, 21(3), 301-310. doi: 10.1002/dac.892
- Saleem, Z., Al-Ghadhban, S., & Al-Naffouri, T. Y. (2012, Nov). On the use of blind source separation for peak detection in spectrum sensing. In *2012 IEEE International Conference on Control System, Computing and Engineering* (p. 66-71). doi: 10.1109/ICC-SCE.2012.6487117
- Sastry, N., Shankar, U., & Wagner, D. (2003). Secure verification of location claims. In *Proceedings of the 2nd ACM workshop on wireless security* (p. 1–10). New York, NY, USA: Association for Computing Machinery. doi: 10.1145/941311.941313
- Schmidt, R. (1986, March). Multiple emitter location and signal parameter estimation. *IEEE Transactions on Antennas and Propagation*, 34(3), 276-280. doi: 10.1109/TAP.1986.1143830
- Sharman, K., Durrani, T., Wax, M., & Kailath, T. (1984, March). Asymptotic performance of eigenstructure spectral analysis methods. In *Icassp '84. IEEE International Conference on Acoustics, Speech, and Signal Processing* (Vol. 9, p. 440-443). doi: 10.1109/ICASSP.1984.1172704

- Shi, J., Yang, D.-S., Shi, S.-G., rui Zhu, Z., & Hu, B. (2017). Spatial time-frequency doa estimation based on joint diagonalization using jacobi rotation. *Applied Acoustics*, 116, 24 - 32. doi: 10.1016/j.apacoust.2016.09.008
- Shiying, T., & Hongqiang, W. (2018, Jan 01). Propagator-based computationally efficient direction finding via low-dimensional equation rooting. *Signal, Image and Video Processing*, 12(1), 83–90. doi: 10.1007/s11760-017-1133-4
- Stoica, P., Händel, P., & Söderström, T. (1995, Nov 01). Study of capon method for array signal processing. *Circuits, Systems and Signal Processing*, 14(6), 749–770. doi: 10.1007/BF01204683
- Stoica, P., & Nehorai, A. (1989, May). Music, maximum likelihood, and cramer-rao bound. *IEEE Transactions on Acoustics, Speech, and Signal Processing*, 37(5), 720-741. doi: 10.1109/29.17564
- Sun, M., Wang, Y., & Pan, J. (2019). Direction of arrival estimation by modified orthogonal propagator method with linear prediction in low snr scenarios. *Signal Processing*, 156, 41 - 45. doi: 10.1016/j.sigpro.2018.10.013
- Tayem, N., Omer, M., Gami, H., & Nayfeh, J. (2013, Nov). Qr-tls esprit for source localization and frequency estimations. In *2013 asilomar conference on signals, systems and computers* (p. 190-194). doi: 10.1109/ACSSC.2013.6810257
- Tian, Z., & Giannakis, G. B. (2006, June). A wavelet approach to wideband spectrum sensing for cognitive radios. In *2006 1st international conference on cognitive radio oriented wireless networks and communications* (p. 1-5). doi: 10.1109/CROWN-COM.2006.363459
- Turqueti, M., Oruklu, E., & Saniie, J. (2014). 17 - smart acoustic sensor array (sasa) system for real-time sound processing applications. In S. Nihtianov & A. Luque (Eds.), *Smart sensors and mems* (p. 492-517). Woodhead Publishing. doi: 10.1533/9780857099297.2.492
- Tzafri, L., & Weiss, A. J. (2016). Application of capon method to direct position determination. *ICT Express*, 2(1), 5 - 9. (Special Issue on Positioning Techniques and Applications) doi: 10.1016/j.icte.2016.02.010
- Vincent, F., Pascal, F., & Besson, O. (2017). A bias-compensated music for small number of samples. *Signal Processing*, 138, 117 - 120. doi: 10.1016/j.sigpro.2017.03.015
- Wan, L., Han, G., Shu, L., Chan, S., & Zhu, T. (2016). The application of doa estimation approach in patient tracking systems with high patient density. *IEEE Transactions on Industrial Informatics*, 12(6), 2353-2364.
- Wang, J., Zhao, Y., & Wang, Z. (2008, May). Low complexity subspace fitting method for wideband signal location. In *2008 5th ifip international confer-*



- ence on wireless and optical communications networks (wocn '08)* (p. 1-4). doi: 10.1109/WOCN.2008.4542533
- Wang, Y., Yang, M., Chen, B., & Xiang, Z. (2016). Improved doa estimation based on real-valued array covariance using sparse bayesian learning. *Signal Processing*, 129, 183 - 189. doi: 10.1016/j.sigpro.2016.06.002
- Wax, M., & Leshem, A. (1996, May). Joint estimation of time delays and directions of arrival of multiple reflections of a known signal. In *1996 ieee international conference on acoustics, speech, and signal processing conference proceedings* (Vol. 5, p. 2622-2625 vol. 5). doi: 10.1109/ICASSP.1996.548002
- Wax, M., Shan, T.-J., & Kailath, T. (1984, August). Spatio-temporal spectral analysis by eigenstructure methods. *IEEE Transactions on Acoustics, Speech, and Signal Processing*, 32(4), 817-827. doi: 10.1109/TASSP.1984.1164400
- Wen, F., & So, H. C. (2015). Tensor-mode for multi-dimensional harmonic retrieval with coherent sources. *Signal Processing*, 108, 530 - 534. doi: 10.1016/j.sigpro.2014.10.009
- Xiao, Z., & Zeng, Y. (2020). *An overview on integrated localization and communication towards 6g*.
- Yan, F.-G., Wang, J., Liu, S., Cao, B., & Jin, M. (2018). Computationally efficient direction of arrival estimation with unknown number of signals. *Digital Signal Processing*, 78, 175 - 184. doi: 10.1016/j.dsp.2018.03.012
- Yoon, Y.-S. (2004, 01). Direction-of-arrival estimation of wideband sources using sensor arrays. In *Phd thesis*. Georgia Institute of Technology.
- Yoon, Y.-S., Kaplan, L., & H. McClellan, J. (2006, 01). Doa estimation of wideband signals.
- Yoon, Y.-S., Kaplan, L. M., & McClellan, J. H. (2006, June). Tops: new doa estimator for wideband signals. *IEEE Transactions on Signal Processing*, 54(6), 1977-1989. doi: 10.1109/TSP.2006.872581
- Yu, H., Liu, J., Huang, Z., Zhou, Y., & Xu, X. (2007, Sept). A new method for wideband doa estimation. In *2007 international conference on wireless communications, networking and mobile computing* (p. 598-601). doi: 10.1109/WICOM.2007.155
- Zeng, Y., Cao, J., Hong, J., Zhang, S., & Xie, L. (2013, Jun 01). Secure localization and location verification in wireless sensor networks: a survey. *The Journal of Supercomputing*, 64(3), 685-701. doi: 10.1007/s11227-010-0501-4
- Zhang, J., Dai, J., & Ye, Z. (2010). An extended tops algorithm based on incoherent signal subspace method. *Signal Processing*, 90(12), 3317 - 3324. doi: 10.1016/j.sigpro.2010.05.031

- Zhang, J., Qiu, T., Song, A., & Tang, H. (2014). A novel correntropy based doa estimation algorithm in impulsive noise environments. *Signal Processing*, 104, 346 - 357. doi: 10.1016/j.sigpro.2014.04.033
- Zhang, P., Lu, J., Wang, Y., & Wang, Q. (2017). Cooperative localization in 5g networks: A survey. *ICT Express*, 3(1), 27 - 32. doi: 10.1016/j.icte.2017.03.005

## **APPENDICES**

## **APPENDIX 1**

### **CURRICULUM VITAE**

#### **PERSONAL INFORMATION**

Surname, Name: Abdelbari, Amr  
Nationality: Egypt  
Date and Place of Birth: 06 February 1993, Sohag  
Marital Status: Married



#### **EDUCATION**

<b>Degree</b>	<b>Institution</b>	<b>Year of Graduation</b>
M.Sc.	Near East University, Nicosia, TRNC, Mersin 10, Turkey, Faculty of Engineering, Department of Electrical & Electronic Engineering	2018
B.Sc.	Sohag University, Sohag, Egypt, Faculty of Engineering, Department of Electrical Engineering	2014

#### **WORK EXPERIENCE**

<b>Year</b>	<b>Place</b>	<b>Enrollment</b>
Feb. 2019 – Present	Department of Electrical and Electronic Engineering, Faculty of Engineering, Near East University, Nicosia, TRNC, Mersin 10, Turkey	Research Assistant
Jul 2015 – Aug 2015	Construction project, Doha, Qatar	Electrical Engineer
Jul 2010 – Feb 2011	Synergy Sohag Center, Sohag, Egypt	Websites Designer

#### **FOREIGN LANGUAGES**

English; fluently spoken and written

#### **HONORS AND AWARDS**

- Register an invention: Design of “ Air Pollution by Solids Ratio “. Registered at Science and Technology Academy, Ministry of Science Research, Egypt.
- 4th place in Robotic Competition: Design of a “Follow-Line Robot” like in factories. The competition was over Egyptian universities. Helwan University, Cairo, Egypt.
- 4th place in Robotic Competition Design of a “Ground Metal Detection Robot”. The competition was over Egyptian universities, GUC University, Cairo, Egypt.

#### **MEMBERSHIP OF PROFESSIONAL ORGANIZATIONS**

- *Member*, IEEE
- *Member*, IEEE Communication Society
- *Member*, Signal Processing Society

#### **PUBLICATIONS IN INTERNATIONAL REFEREED JOURNALS (IN COVERAGE OF SCI/SCI-EXPANDED**

- Bilgehan, B., & Abdelbari, A. (2019). Fast detection and DOA estimation of the unknown wideband signal sources. *International Journal of Communication Systems*, 32(11), e3968. (e3968 dac.3968) doi: 10.1002/dac.3968
- Haci, H., & Abdelbari, A. (2020). Throughput enhanced scheduling (TES) scheme for ultra-dense networks. *International Journal of Communication Systems*, 33(4), e4229. (e4229 dac.4229) doi: 10.1002/dac.4229
- Abdelbari, A., & Bilgehan, B. (2020). A probabilistic-based approach for direction-of-arrival estimation and localization of multiple sources. *International Journal of Communication Systems*, 33(11), e4425. (e4425 dac.4425) doi: 10.1002/dac.4425
- Abdelbari, A., & Bilgehan, B. (2021). PESO: probabilistic evaluation of subspaces orthogonality for wideband DOA estimation. *Multidimens. Syst. Signal Process.*, 32(2), 715–746. doi: 10.1007/s11045-020-00757-6

#### **PUBLICATIONS PRESENTED IN INTERNATIONAL ACADEMIC CONFERENCES AND PUBLISHED IN PROCEEDING BOOKS (IN COVERAGE OF WEB OF SCI-**

## ENCE AND SCOPUS

- Hacı, H., & Abdelbari, A. (2019). A novel scheduling scheme for ultra-dense networks. In *2019 international symposium on networks, computers and communications (ISNCC)* (p. 1-6). doi: 10.1109/ISNCC.2019.8909118
- Abdelbari, A., & Hacı, H. (2019a). Fuzzy logic-based user scheduling scheme for 5G wireless networks and beyond. In *International conference on theory and application of soft computing, computing with words and perceptions* (pp. 429–435).
- Bilgehan, B., & Abdelbari, A. (2019b). A novel DOA estimation method for wideband sources based on fuzzy systems. In *International conference on theory and application of soft computing, computing with words and perceptions* (pp. 405–412).
- Abdelbari, A., & Hacı, H. (2019b). An opportunistic user scheduling scheme for ultra-dense wireless networks. In *2019 11th international conference on electrical and electronics engineering (ELECO)* (p. 1080-1084). doi: 10.23919/ELECO47770.2019.8990469
- Abdelbari, A., & Bilgehan, B. (2020a). A novel DOA estimation method of several sources for 5G networks. In *2020 international conference on electrical, communication, and computer engineering (ICECCE)* (p. 1-6). doi: 10.1109/ICECCE49384.2020.9179306
- Naser, N., & Abdelbari, A. (2020). Estimation of global solar radiation using back propagation neural network: A case study Tripoli, Libya. In *2020 international conference on electrical, communication, and computer engineering (ICECCE)* (p. 1-5). doi: 10.1109/ICECCE49384.2020.9179201

## THESES

### Master

- Abdelbari, A. (2018). *Direction of arrival estimation of wideband RF sources*. (Unpublished master's thesis). Near East University.

### Undergraduate

- Abdelbari, A. (2014). *Design of RFID-Based Security System*. Undergraduate project (B.Sc.). Sohag University, Sohag, Egypt.

## **COURSES GIVEN** *(from 2019 to 2021)*

### *Undergraduate*

- Technical Drawing and Electrical applications.
- Microprocessors (Lab).
- Electrical Measurements (lab).
- Communication Systems (lab).
- Electronics II (Lecture).
- Signals & Systems (Lab & Tutorial).
- Machine Learning (Lab).
- Signals & Systems (Lecture and Lab).
- Introduction to Electronics (Lecture).
- Introduction to Electric and Electronics (Lecture).
- Communication Systems (lab).
- Electromagnetic Theory (Lecture).
- Electronics I (Lecture).
- Communication Systems (Lecture).
- Electrical Measurements and Instruments (Lecture).

## **HOBBIES**

Reading, coding, drawing, and exploring new things & places.

## **OTHER INTERESTS**

Signal processing, Array signal processing, Wireless communications, Networks

## APPENDIX 2

### SIMILARITY REPORT

<div><div>turnitin</div><div>Originality Report</div></div> <div>Document Viewer</div>	<div>Processed on: 02-Mar-2022 11:57 EET</div> <div>ID: 1773255538</div> <div>Word Count: 345</div> <div>Submitted: 2</div>	<div>Abstract</div> <div>By Amr Abdelbari</div>	<div><div>Similarity Index</div><div>0%</div></div> <div><div>Similarity by Source</div><div>Internet Sources: 0%</div><div>Publications: 0%</div><div>Student Papers: 0%</div></div>
<div><div>turnitin</div><div>Originality Report</div></div> <div>Document Viewer</div>	<div>Processed on: 02-Mar-2022 12:02 EET</div> <div>ID: 1773255538</div> <div>Word Count: 2465</div> <div>Submitted: 3</div>	<div>Introduction</div> <div>By Amr Abdelbari</div>	<div><div>Similarity Index</div><div>0%</div></div> <div><div>Similarity by Source</div><div>Internet Sources: 0%</div><div>Publications: 0%</div><div>Student Papers: 0%</div></div>
<div><div>turnitin</div><div>Originality Report</div></div> <div>Document Viewer</div>	<div>Processed on: 02-Mar-2022 12:07 EET</div> <div>ID: 1773255538</div> <div>Word Count: 7134</div> <div>Submitted: 4</div>	<div>Chapter 2</div> <div>By Amr Abdelbari</div>	<div><div>Similarity Index</div><div>36%</div></div> <div><div>Similarity by Source</div><div>Internet Sources: 0%</div><div>Publications: 36%</div><div>Student Papers: 0%</div></div>
<div><div>turnitin</div><div>Originality Report</div></div> <div>Document Viewer</div>	<div>Processed on: 03-Mar-2022 12:07 EET</div> <div>ID: 1773255538</div> <div>Word Count: 3557</div> <div>Submitted: 5</div>	<div>Chapter 3</div> <div>By Amr Abdelbari</div>	<div><div>Similarity Index</div><div>0%</div></div> <div><div>Similarity by Source</div><div>Internet Sources: 0%</div><div>Publications: 0%</div><div>Student Papers: 0%</div></div>
<div><div>turnitin</div><div>Originality Report</div></div> <div>Document Viewer</div>	<div>Processed on: 04-Mar-2022 12:07 EET</div> <div>ID: 1773255538</div> <div>Word Count: 476</div> <div>Submitted: 6</div>	<div>Conclusion</div> <div>By Amr Abdelbari</div>	<div><div>Similarity Index</div><div>0%</div></div> <div><div>Similarity by Source</div><div>Internet Sources: 0%</div><div>Publications: 0%</div><div>Student Papers: 0%</div></div>
<div><div>turnitin</div><div>Originality Report</div></div> <div>Document Viewer</div>	<div>Processed on: 28-Feb-2022 23:25 EET</div> <div>ID: 1773255538</div> <div>Word Count: 19160</div> <div>Submitted: 1</div>	<div>full thesis</div> <div>By Amr Abdelbari</div>	<div><div>Similarity Index</div><div>26%</div></div> <div><div>Similarity by Source</div><div>Internet Sources: 0%</div><div>Publications: 26%</div><div>Student Papers: 0%</div></div>
<div><div>turnitin</div><div>Originality Report</div></div> <div>Document Viewer</div>	<div>Processed on: 07-Mar-2022 11:39 EET</div> <div>ID: 1778429996</div> <div>Word Count: 15831</div> <div>Submitted: 1</div>	<div>Thesis without References</div> <div>By Amr Abdelbari</div>	<div><div>Similarity Index</div><div>27%</div></div> <div><div>Similarity by Source</div><div>Internet Sources: 0%</div><div>Publications: 27%</div><div>Student Papers: 0%</div></div>